

# The MCMC split sampler: A block Gibbs sampling scheme for latent Gaussian models

Óli Páll Geirsson, Birgir Hrafnkelsson and Helgi Sigurðarson

Department of Mathematics

Faculty of Physical Sciences

School of Engineering and Natural Sciences

University of Iceland

and

Daniel Simpson

Department of Statistics

University of Warwick, Coventry

November 15, 2021

## Abstract

A novel computationally efficient Markov chain Monte Carlo (MCMC) scheme for latent Gaussian models (LGMs) is proposed in this paper. The sampling scheme is a two block Gibbs sampling scheme designed to exploit the model structure of LGMs. We refer to the proposed sampling scheme as the MCMC split sampler. The principle idea behind the MCMC split sampler is to split the latent Gaussian parameters into two vectors. The former vector consists of latent parameters which appear in the data density function, while the latter vector consists of latent parameters which do not appear in it. The former vector is placed in the first block of the proposed sampling scheme and the latter vector is placed in the second block along with any potential hyperparameters. The resulting conditional posterior density functions within the blocks allow the MCMC split sampler to handle, by design, LGMs with latent models imposed on more than just the mean structure of the data density function. The MCMC split sampler is also designed to be applicable for any choice of a parametric data density function. Moreover, it scales well in terms of computational efficiency when the dimension of the latent model increase.

## 1 Introduction

Latent Gaussian models (LGMs) form a flexible subclass of Bayesian hierarchical models and have become popular in many areas of statistics and various fields of applications, as LGMs are practical from a statistical modeling point of view and readily interpretable. For example, LGMs play an important role in spatial statistics, see Cressie [1993], Diggle et al. [1998], Delfiner et al. [2009]; statistical climatology [Cooley et al., 2007, Guttorp

and Gneiting, 2006]; disease mapping [Pettitt et al., 2002, Lawson, 2013]; stochastic volatility models [Martino et al., 2011]; and hydrology [Schaeffli et al., 2007], to name a few. Moreover, LGMs can be viewed as a specific extension of structured additive regression models [Fahrmeir et al., 1994, Rue et al., 2009], in the sense that, the data density function of each data point can depend on more than a single linear functional of the latent field through more than just the mean structure, as discussed in Martins et al. [2013].

Although LGMs are well suited from a statistical modeling point of view their posterior inference becomes computationally challenging when latent models are desired for more than just the mean structure of the data density function [Martins et al., 2013], when the number of parameters associated with the latent model increase; or when the data density function is non-Gaussian. The aim of this paper is to propose a novel computationally efficient Markov chain Monte Carlo (MCMC) scheme which serves to address these computational issues. The proposed sampling scheme is referred to as the *MCMC split sampler* in this paper. It is designed to handle LGMs where latent models are imposed on more than just the mean structure of the likelihood. It scales well in terms of computational efficiency when the dimensions of the latent models increase and it is applicable for any choice of a parametric data density function. The main novelty of the MCMC split sampler lies in how the model parameters of a LGM are split into two blocks. As a result of the proposed blocking scheme, one of the blocks exploits the latent Gaussian structure in a natural way and becomes invariant of the data density function.

Markov chain Monte Carlo (MCMC) methods form the backbone of modern Bayesian posterior inference and are, in principle, applicable to almost any Bayesian model. However, the mixing and convergence properties of the MCMC chains can be poor for involved models structures and large data sets if parameters that are dependent in the posterior are not dealt with properly, see for example Murray and Adams [2010]. In particular, the mixing and convergence properties of the popular single site updating strategy can be extremely poor due to strong dependencies of parameters in the posterior distribution as discussed in Knorr-Held and Rue [2002]. Several MCMC sampling strategies have been suggested for Bayesian hierarchical models to improve the mixing properties of MCMC algorithms. For example, methods based on approximate diffusions such as the Metropolis Adjusted Langevin algorithm (MALA), see Roberts and Rosenthal [1998]; methods based on Hamiltonian mechanics (HMC), suggested by Neal [1993], which use the gradient of the target density to drive the proposal mechanism toward regions of higher posterior density; manifold methods, proposed by Girolami and Calderhead [2011], which provide a systematic way of designing proposal densities for MALA and HMC by making use of the gradient and curvature information of the target density; and various block sampling strategies such as the one block updating strategy of Knorr-Held and Rue [2002]. Filippone et al. [2013] conducted a detailed comparison of these methods for LGMs and found that the single block strategy of Knorr-Held and Rue [2002], in which the latent field and its corresponding hyperparameters are updated jointly in a single block, performed best in most situations. Furthermore, by using numerical methods for fast sampling of Gaussian Markov random fields (GMRFs) [Rue, 2001], the single block sampler can be

implemented with a low computational cost for LGMs. However, using only a single block sampler for LGMs with a non-Gaussian likelihood and high dimensional latent fields can be problematic, as parameters accepted in regions of low posterior probability can cause the MCMC chain to get stuck.

Alternative to MCMC methods are deterministic approximate posterior inference methods, such as the Integrated nested Laplace approximation (INLA) [Rue et al., 2009]. INLA is a fast approximate inference method for LGMs in which the data density of each data point only depends on a single linear functional of the latent field. While this assumption holds in many practical cases, there are many models in which we want the latent field to enter the data density of a single observation through two or more parameters, see Kneib [2013] and Martins et al. [2013] for further discussion. For example in Hrafinkelsson et al. [2012] and Geirsson et al. [2015], latent Gaussian spatial models were imposed on the location, scale and shape structure of the data density function.

The MCMC split sampler is a two block Gibbs sampling scheme [Geman and Geman, 1984, Casella and George, 1992] designed for LGMs, which addresses the aforementioned inference problems. The MCMC split sampler is based on the following model setup for LGMs, to which we adhere to in this paper.

**Data-level:** The observations  $\mathbf{y}$  depend on the latent field  $\mathbf{x}$ , through some choice of data distribution with a data density function  $\pi(\mathbf{y} \mid \mathbf{x})$ .

**Latent level:** The prior for the latent field  $\mathbf{x}$  is Gaussian and is potentially dependent on hyperparameters  $\boldsymbol{\theta}$ , with a density function

$$\pi(\mathbf{x} \mid \boldsymbol{\theta}) = \mathcal{N}(\mathbf{x} \mid \boldsymbol{\mu}(\boldsymbol{\theta}), \mathbf{Q}(\boldsymbol{\theta})^{-1}).$$

**Hyperparameter level:** A prior distribution is assigned for the hyperparameters  $\boldsymbol{\theta}$ , with a density function  $\pi(\boldsymbol{\theta})$ .

The principle idea behind the MCMC split sampler is to split the latent Gaussian parameters  $\mathbf{x}$  into two vectors,  $\boldsymbol{\eta}$  and  $\boldsymbol{\nu}$ , where  $\boldsymbol{\eta}$  consists of elements that appear in the data density function and  $\boldsymbol{\nu}$  consists of elements that do not appear in it. Thus, the data  $\mathbf{y}$  become conditionally independent of  $(\boldsymbol{\nu}, \boldsymbol{\theta})$  conditioned on  $\boldsymbol{\eta}$ , that is,  $\pi(\mathbf{y} \mid \mathbf{x}, \boldsymbol{\theta}) = \pi(\mathbf{y} \mid \boldsymbol{\eta})$ . For the posterior inference, all the model parameters are grouped into two blocks. That is,  $\boldsymbol{\eta}$  is placed in a block we refer to as the *data-rich* block in this paper, while both  $\boldsymbol{\nu}$  and the hyperparameters  $\boldsymbol{\theta}$  are placed in another block referred to as the *data-poor* block. A Gibbs sampling strategy is then implemented for each block, conditioned on the other block.

In many practical applications with non-Gaussian data density functions, especially in the field of spatial statistics, the vector  $\boldsymbol{\eta}$  in the data-rich block has a complicated but low-dimensional conditional posterior structure, while the parameter vector  $\boldsymbol{\nu}$  in the data-poor block is often of much higher dimension than that of the parameters in the data-poor block [Hrafinkelsson et al., 2012]. Therefore, by using the proposed blocking scheme the potentially computationally demanding conditional posterior density in the data-rich block contains a minimum number of necessary parameters. Furthermore, the

conditional posterior density of  $\boldsymbol{\nu}$  becomes conditionally Gaussian conditioned on the parameter vector  $\boldsymbol{\eta}$  and the hyperparameters  $\boldsymbol{\theta}$ . This designed structure, that is, the minimal dimension of the parameters in the data-rich block and the conditional Gaussian posterior structure within the data-poor block, is exploited to implement computationally efficient sampling schemes within the blocks. Further, the proposed scheme scales well when the dimension of  $\boldsymbol{\nu}$  increases, as discussed in the ensuing paragraph.

The MCMC split sampler is modular by design such that, in principle, any efficient MCMC sampler can be implemented for each block. In this paper, we propose computationally efficient sampling strategies that are tailored to the particular conditional model structure of each block. Within the data-rich block we present a strategy based on the gradient and curvature information of the target density that results in an independence proposal mechanism as discussed in Rue and Held [2005]. Conditional independence resulting from the model structure within the block can be utilized in some cases to increase acceptance in the Metropolis-Hastings algorithm [Metropolis et al., 1953, Hastings, 1970]. In order to update the data-poor block, a modified version of the fast single block updater of Knorr-Held and Rue [2002] is proposed, which exploits the fact that the conditional posterior of the vector  $\boldsymbol{\nu}$  is Gaussian conditioned on  $\boldsymbol{\eta}$  and  $\boldsymbol{\theta}$ . This step is invariant of the choice of a data density function as the data-poor block is updated conditioned on the data-rich block. Moreover, if the latent field  $\boldsymbol{x}$  is a GMRF with a sparse precision structure, the sampling strategy for the data-poor block is shown to conserve the sparse GMRF precision structure, allowing for fast sampling of the corresponding GMRF.

The paper is organized as follows. Section 2.1 and Section 2.2 are devoted to the motivation, introduction and the setup of the MCMC split sampler. The proposed sampling schemes within the data-rich and data-poor blocks are presented in Sections 2.3 and Section 2.4, respectively. Examples on the implementation of the MCMC split sampler are given in Section 3. In Section 3.1 we present a LGM with a latent spatial model structure on mean and log-variance parameters, and show how the MCMC split sampler scales well as the dimensions of the latent parameters in the data-poor block increase. An example on extremes based on a simulated data set is given in Section 3.2, where the focus is on a LGM where latent models are imposed on all three parameters of the generalized extreme value distribution. In Appendix A, we give an extension to the sampling scheme proposed in Section 2.3, which is applicable if conditional independence assumptions are imposed on the data density function. Lastly, in Appendix B, we show the necessary proofs for the main results in the paper.

## 2 The MCMC split sampler

### 2.1 Motivation and model setup

Consider, as a motivation and without loss of generality, a data density function  $\pi(\mathbf{y} \mid \boldsymbol{\mu}, \boldsymbol{\tau})$  where  $\boldsymbol{\mu}$  and  $\boldsymbol{\tau}$  are vectors of location and log-scale parameters, respectively, which are modeled with latent Gaussian fields. That is, assume the following additive model

structure

$$\boldsymbol{\mu} = \mathbf{X}_\mu \boldsymbol{\beta}_\mu + \mathbf{A}_\mu \mathbf{u}_\mu, \quad \boldsymbol{\tau} = \mathbf{X}_\tau \boldsymbol{\beta}_\tau + \mathbf{A}_\tau \mathbf{u}_\tau$$

where  $\mathbf{X}_\mu$  and  $\mathbf{X}_\tau$  are fixed design matrices;  $\boldsymbol{\beta}_\mu$  and  $\boldsymbol{\beta}_\tau$  are the corresponding weights;  $\mathbf{A}_\mu$  and  $\mathbf{A}_\tau$  are fixed matrices; and  $\mathbf{u}_\mu$  and  $\mathbf{u}_\tau$  are structured random effects. In order to increase computational stability in the posterior inference calculations and for mathematical derivations of the MCMC split sampler, we introduce unstructured random effects,  $\boldsymbol{\epsilon}_\mu$  and  $\boldsymbol{\epsilon}_\tau$ , to the model. That is,

$$\boldsymbol{\mu} = \mathbf{X}_\mu \boldsymbol{\beta}_\mu + \mathbf{A}_\mu \mathbf{u}_\mu + \boldsymbol{\epsilon}_\mu, \quad \boldsymbol{\tau} = \mathbf{X}_\tau \boldsymbol{\beta}_\tau + \mathbf{A}_\tau \mathbf{u}_\tau + \boldsymbol{\epsilon}_\tau. \quad (2.1)$$

Small variances can be imposed *a priori* on the unstructured random effects  $\boldsymbol{\epsilon}_\mu$  and  $\boldsymbol{\epsilon}_\tau$  if they are not desired in the model. However, adding the unstructured random effects is reasonable in many cases from a statistical modeling point of view as they serve as error terms for the latent models. Furthermore, adding the  $\boldsymbol{\epsilon}_\mu$  and  $\boldsymbol{\epsilon}_\tau$  terms to the latent models yields an analogous latent model structure as implied by the structured additive regression in Fahrmeir et al. [1994] where only the mean is linked to a structured additive predictor through a link function.

Assign the following Gaussian prior density functions to the latent model parameters

$$\begin{aligned} \pi(\boldsymbol{\beta}_\mu) &= \mathcal{N}(\boldsymbol{\beta}_\mu \mid \boldsymbol{\mu}_{\mu\beta}, \mathbf{Q}_{\mu\beta}^{-1}), & \pi(\boldsymbol{\beta}_\tau) &= \mathcal{N}(\boldsymbol{\beta}_\tau \mid \boldsymbol{\mu}_{\tau\beta}, \mathbf{Q}_{\tau\beta}^{-1}) \\ \pi(\mathbf{u}_\mu) &= \mathcal{N}(\mathbf{u}_\mu \mid \boldsymbol{\mu}_{\mu u}, \mathbf{Q}_{\mu u}^{-1}), & \pi(\mathbf{u}_\tau) &= \mathcal{N}(\mathbf{u}_\tau \mid \boldsymbol{\mu}_{\tau u}, \mathbf{Q}_{\tau u}^{-1}) \\ \pi(\boldsymbol{\epsilon}_\mu) &= \mathcal{N}(\boldsymbol{\epsilon}_\mu \mid \mathbf{0}, \mathbf{Q}_{\mu\epsilon}^{-1}), & \pi(\boldsymbol{\epsilon}_\tau) &= \mathcal{N}(\boldsymbol{\epsilon}_\tau \mid \mathbf{0}, \mathbf{Q}_{\tau\epsilon}^{-1}) \end{aligned} \quad (2.2)$$

where parameters of the prior density functions can potentially depend of a set of hyper-parameters  $\boldsymbol{\theta}$ , and  $\mathbf{Q}_{\mu\epsilon}^{-1}$  and  $\mathbf{Q}_{\tau\epsilon}^{-1}$  are diagonal matrices.

As the vector  $\boldsymbol{\mu}$  in equation (2.1) is a linear combination of  $\boldsymbol{\beta}_\mu$ ,  $\mathbf{u}_\mu$  and  $\boldsymbol{\epsilon}_\mu$ , it is equivalent to obtain MCMC samples from the posterior distribution of  $(\boldsymbol{\mu}, \boldsymbol{\beta}_\mu, \mathbf{u}_\mu)$  and from the posterior distribution of  $(\boldsymbol{\beta}_\mu, \mathbf{u}_\mu, \boldsymbol{\epsilon}_\mu)$ . Analogous argument holds for the log-scale parameters. The MCMC split sampler is designed to obtain MCMC samples from the posterior distribution of  $(\boldsymbol{\mu}, \boldsymbol{\tau}, \boldsymbol{\beta}_\mu, \boldsymbol{\beta}_\tau, \mathbf{u}_\mu, \mathbf{u}_\tau)$  as opposed to  $(\boldsymbol{\beta}_\mu, \boldsymbol{\beta}_\tau, \mathbf{u}_\mu, \mathbf{u}_\tau, \boldsymbol{\epsilon}_\mu, \boldsymbol{\epsilon}_\tau)$  as in the former parameterization only the vector  $(\boldsymbol{\mu}, \boldsymbol{\tau})$  enters the data density function, while all the elements of the latter vector enter the data density function in the latter parameterization. This parameterization for posterior inference is along the lines of the posterior inference scheme proposed in Rue et al. [2009]. Thus, define

$$\boldsymbol{\eta} = (\boldsymbol{\mu}, \boldsymbol{\tau})^\top, \quad \boldsymbol{\nu} = (\boldsymbol{\beta}_\mu, \mathbf{u}_\mu, \boldsymbol{\beta}_\tau, \mathbf{u}_\tau)^\top$$

which will act as the splitting of the parameters of the latent field.

The latent model structure in (2.1) and the prior distributions in (2.2) can be written in a joint matrix form, which forms the basis for the derivation of the MCMC split sampler. Define the following matrices and vectors

$$\mathbf{Z} = \begin{pmatrix} \mathbf{X}_\mu & \mathbf{A}_\mu & \cdot & \cdot \\ \cdot & \cdot & \mathbf{X}_\tau & \mathbf{A}_\tau \end{pmatrix}, \quad \boldsymbol{\epsilon} = \begin{pmatrix} \boldsymbol{\epsilon}_\mu \\ \boldsymbol{\epsilon}_\tau \end{pmatrix}, \quad \mathbf{Q}_\epsilon = \begin{pmatrix} \mathbf{Q}_{\mu\epsilon} & \cdot \\ \cdot & \mathbf{Q}_{\tau\epsilon} \end{pmatrix}$$

and group the following parameters and matrices together

$$\boldsymbol{\mu}_\nu = \begin{pmatrix} \boldsymbol{\mu}_{\mu\beta} \\ \boldsymbol{\mu}_{\mu u} \\ \boldsymbol{\mu}_{\tau\beta} \\ \boldsymbol{\mu}_{\tau u} \end{pmatrix}, \quad \mathbf{Q}_\nu = \begin{pmatrix} \mathbf{Q}_{\mu\beta} & \cdot & \cdot & \cdot \\ \cdot & \mathbf{Q}_{\mu u} & \cdot & \cdot \\ \cdot & \cdot & \mathbf{Q}_{\tau\beta} & \cdot \\ \cdot & \cdot & \cdot & \mathbf{Q}_{\tau u} \end{pmatrix}$$

where the dotted entries denote zero entries. The additive model structure implied by (2.1) for both latent parameters is thus equivalent to the matrix form

$$\boldsymbol{\eta} = \mathbf{Z}\boldsymbol{\nu} + \boldsymbol{\epsilon} \quad (2.3)$$

and the Gaussian prior assumptions in (2.2) are equivalent to

$$\begin{aligned} \pi(\boldsymbol{\eta} \mid \boldsymbol{\nu}) &= \mathcal{N}(\boldsymbol{\eta} \mid \mathbf{Z}\boldsymbol{\nu}, \mathbf{Q}_\epsilon^{-1}), \\ \pi(\boldsymbol{\nu}) &= \mathcal{N}(\boldsymbol{\nu} \mid \boldsymbol{\mu}_\nu, \mathbf{Q}_\nu^{-1}). \end{aligned} \quad (2.4)$$

As the data density function and the corresponding parameters were arbitrarily chosen above, analogous derivations can be carried out for any parametric data density function and any of its parameters. For example, in addition to imposing latent Gaussian models on the location and log-scale parameters of the generalized extreme value distribution a latent Gaussian model can also be imposed on the shape parameter, see Section 3.2 for details. Therefore, equations (2.3) and (2.4) are general in the sense that most of LGMs used in practice can be expressed in the same form. We will thus adapt equations (2.3) and (2.4) as a general setup for the latent model structures for LGMs henceforth in this paper.

The following lemma, based on known results, plays a vital role in the implementation of the MCMC split sampler.

**Lemma 1.** *Assume the distribution assumptions given in (2.4), for any mean vector  $\boldsymbol{\mu}_\nu$ , fixed matrix  $\mathbf{Z}$ , and precision matrices  $\mathbf{Q}_\epsilon$  and  $\mathbf{Q}_\nu$ . The joint prior density function of  $(\boldsymbol{\eta}, \boldsymbol{\nu})$  is then Gaussian of the form*

$$\pi \begin{pmatrix} \boldsymbol{\eta} \\ \boldsymbol{\nu} \end{pmatrix} = \mathcal{N} \left( \begin{pmatrix} \boldsymbol{\eta} \\ \boldsymbol{\nu} \end{pmatrix} \mid \begin{pmatrix} \mathbf{Z}\boldsymbol{\mu}_\nu \\ \boldsymbol{\mu}_\nu \end{pmatrix}, \begin{pmatrix} \mathbf{Q}_\epsilon & -\mathbf{Q}_\epsilon \mathbf{Z} \\ -\mathbf{Z}^\top \mathbf{Q}_\epsilon & \mathbf{Q}_\nu + \mathbf{Z}^\top \mathbf{Q}_\epsilon \mathbf{Z} \end{pmatrix}^{-1} \right) \quad (2.5)$$

and the conditional density function of  $\boldsymbol{\nu}$  conditioned on  $\boldsymbol{\eta}$  becomes

$$\pi(\boldsymbol{\nu} \mid \boldsymbol{\eta}) = \mathcal{N} \left( \boldsymbol{\nu} \mid \mathbf{Q}_{\nu|\eta}^{-1} (\mathbf{Q}_\nu \boldsymbol{\mu}_\nu + \mathbf{Z}^\top \mathbf{Q}_\epsilon \boldsymbol{\eta}), \mathbf{Q}_{\nu|\eta}^{-1} \right) \quad (2.6)$$

where  $\mathbf{Q}_{\nu|\eta} = \mathbf{Q}_\nu + \mathbf{Z}^\top \mathbf{Q}_\epsilon \mathbf{Z}$ .

See Appendix B.1 for proof. Note that, as the vector  $(\boldsymbol{\eta}, \boldsymbol{\nu})$  is jointly Gaussian it can be viewed as the latent Gaussian vector  $\boldsymbol{x}$  in the LGM setup.

## 2.2 The sampling scheme

The vector  $\boldsymbol{\eta}$  in (2.3) consists of the parameters of the latent field that explicitly enter the likelihood function while the vector  $\boldsymbol{\nu}$  consists of the parameters of the latent field which do not enter it. Therefore, the data vector  $\mathbf{y}$  is conditionally independent of  $\boldsymbol{\nu}$  conditioned on  $\boldsymbol{\eta}$ , that is  $\pi(\mathbf{y} \mid \boldsymbol{\eta}, \boldsymbol{\nu}) = \pi(\mathbf{y} \mid \boldsymbol{\eta})$ . The parameters  $\boldsymbol{\eta}$  and  $\boldsymbol{\nu}$  are referred to as the data-rich and data-poor components of the latent field, respectively, in this paper. The corresponding posterior distribution, where the data-poor components of the latent field are potentially dependent on a vector of hyperparameters  $\boldsymbol{\theta}$ , is thus proportional to

$$\pi(\boldsymbol{\eta}, \boldsymbol{\nu}, \boldsymbol{\theta} \mid \mathbf{y}) \propto \pi(\mathbf{y} \mid \boldsymbol{\eta})\pi(\boldsymbol{\eta}, \boldsymbol{\nu} \mid \boldsymbol{\theta})\pi(\boldsymbol{\theta}). \quad (2.7)$$

Using the relationship in (2.7), we propose the following two block MCMC sampling scheme to obtain MCMC samples from the posterior density  $\pi(\boldsymbol{\eta}, \boldsymbol{\nu}, \boldsymbol{\theta} \mid \mathbf{y})$ . The vector  $\boldsymbol{\eta}$  is placed in the data-rich block, and the vectors  $\boldsymbol{\nu}$  and  $\boldsymbol{\theta}$  are grouped together in the data-poor block. The MCMC split sampler obtains a sample from the posterior density  $\pi(\boldsymbol{\eta}, \boldsymbol{\nu}, \boldsymbol{\theta} \mid \mathbf{y})$  by sampling from one of the blocks conditioned on the other in a Gibbs sampling setting. That is, the  $(k + 1)$ -th MCMC sample from the posterior density  $\pi(\boldsymbol{\eta}, \boldsymbol{\nu}, \boldsymbol{\theta} \mid \mathbf{y})$  is obtained by using the following two block Gibbs sampling scheme

**Data-rich block:** sample  $\boldsymbol{\eta}^{k+1}$  from  $\pi(\boldsymbol{\eta} \mid \mathbf{y}, \boldsymbol{\nu}^k, \boldsymbol{\theta}^k)$

**Data-poor block:** sample  $(\boldsymbol{\nu}^{k+1}, \boldsymbol{\theta}^{k+1})$  jointly from  $\pi(\boldsymbol{\nu}, \boldsymbol{\theta} \mid \mathbf{y}, \boldsymbol{\eta}^{k+1})$

This scheme forms the basis of the MCMC split sampler. The potentially involved but often low-dimensional structure of the data-rich block is separated from the parameters in the data-poor block. By separating the two blocks, MCMC sampling strategies which exploit the conditional model structures can be implemented within each block in order to increase computational efficiency. Although any computationally efficient MCMC samplers are applicable within the blocks, we propose the following sampling schemes which are tailored for the conditional model structures of the blocks. The details of the proposed samplers for each block are summarized in Section 2.3 and Section 2.4.

## 2.3 Sampler for the data-rich block

The conditional posterior density function  $\pi(\boldsymbol{\eta} \mid \mathbf{y}, \boldsymbol{\nu}, \boldsymbol{\theta})$  in the data-rich block is intractable in most applications. In order to obtain MCMC samples from the conditional posterior density function we propose the following Metropolis–Hasting type MCMC algorithm with a tailored independence proposal density [Rue and Held, 2005].

To construct a computationally efficient independence proposal density, we approximate the conditional posterior density  $\pi(\boldsymbol{\eta} \mid \mathbf{y}, \boldsymbol{\nu}, \boldsymbol{\theta})$  with a Gaussian approximation evaluated at the mode of conditional posterior density. Using the logarithm of the conditional posterior, that is

$$\log \pi(\boldsymbol{\eta} \mid \mathbf{y}, \boldsymbol{\nu}, \boldsymbol{\theta}) = f(\boldsymbol{\eta}) - \frac{1}{2}\boldsymbol{\eta}^\top \mathbf{Q}_\epsilon \boldsymbol{\eta} + (\mathbf{Q}_\epsilon \mathbf{Z}\boldsymbol{\nu})^\top \boldsymbol{\eta} + \text{const} \quad (2.8)$$

where  $f(\boldsymbol{\eta}) = \log \pi(\mathbf{y} \mid \boldsymbol{\eta})$  for notational convenience, the following can be shown.

**Theorem 2.** *The Gaussian approximation of the conditional posterior density  $\pi(\boldsymbol{\eta} \mid \mathbf{y}, \boldsymbol{\nu}, \boldsymbol{\theta})$  is given by*

$$\tilde{\pi}(\boldsymbol{\eta} \mid \mathbf{y}, \boldsymbol{\nu}, \boldsymbol{\theta}) = \mathcal{N}(\boldsymbol{\eta} \mid \boldsymbol{\eta}^0, (\mathbf{Q}_\epsilon - \mathbf{H})^{-1}) \quad (2.9)$$

where  $\boldsymbol{\eta}^0$  is the mode of the conditional posterior density  $\pi(\boldsymbol{\eta} \mid \mathbf{y}, \boldsymbol{\nu}, \boldsymbol{\theta})$  and  $\mathbf{H}$  is the Hessian of the logarithm of conditional posterior evaluated at the mode,  $\mathbf{H} = \nabla^2 f(\boldsymbol{\eta}^0)$ .

See Appendix B.1 for proof. Note that, adding the additive unstructured error term  $\boldsymbol{\epsilon}$  to the model in (2.2) prevents the the precision matrix in (2.9) from being singular and thus ensures numerical stability.

As the Gaussian approximation in (2.9) is constructed at the conditional posterior mode  $\boldsymbol{\eta}^0$ , a proposal density  $q$  for  $\boldsymbol{\eta}$  based on (2.9) thus becomes invariant of the current position of  $\boldsymbol{\eta}$  in the MCMC iteration. Therefore, the proposal density  $q$  is an independence proposal density [Chib and Greenberg, 1995, Rue and Held, 2005]. That is, in the  $(k + 1)$ -th iteration the proposal density is invariant of  $\boldsymbol{\eta}^k$ , that is  $q(\boldsymbol{\eta}^* \mid \boldsymbol{\eta}^k) = q(\boldsymbol{\eta}^*)$ .

When a new  $\boldsymbol{\eta}^*$  is proposed with the independence proposal density in (2.9) in the  $(k + 1)$ -th iteration, it is accepted with probability

$$\alpha = \min \left\{ 1, \frac{\pi(\boldsymbol{\eta}^* \mid \mathbf{y}, \boldsymbol{\nu}, \boldsymbol{\theta})}{\pi(\boldsymbol{\eta}^k \mid \mathbf{y}, \boldsymbol{\nu}, \boldsymbol{\theta})} \cdot \frac{q(\boldsymbol{\eta}^k)}{q(\boldsymbol{\eta}^*)} \right\}. \quad (2.10)$$

The logarithm of the ratio in (2.10) can be simplified, as stated in Lemma 3, in order to reduce computational cost.

**Lemma 3.** *Assume the proposal density  $q$  implied by the Gaussian approximation in (2.9) for the data-rich block. The logarithm of the acceptance ratio given in (2.10) can be simplified to*

$$r = f(\boldsymbol{\eta}^*) - \left( \frac{1}{2}(\boldsymbol{\eta}^*)^\top \mathbf{H} + \mathbf{b}^\top \right) \boldsymbol{\eta}^* - f(\boldsymbol{\eta}^k) + \left( \frac{1}{2}(\boldsymbol{\eta}^k)^\top \mathbf{H} + \mathbf{b}^\top \right) \boldsymbol{\eta}^k \quad (2.11)$$

where  $\mathbf{b} = \nabla f(\boldsymbol{\eta}^0) - \mathbf{H}\boldsymbol{\eta}^0$ .

See Appendix B.2 for proof. As the gradient  $\nabla f(\boldsymbol{\eta}^0)$  and Hessian  $\mathbf{H}$  have already been calculated to obtain (2.9), the expression in (2.11) is computationally efficient to calculate.

In many applications conditional independence assumptions are imposed on the data density function. That is, there exists a partition of  $\boldsymbol{\eta}$  into subvectors  $\boldsymbol{\eta}_i$ , such that  $\pi(\mathbf{y} \mid \boldsymbol{\eta}) = \prod_i \pi_i(\mathbf{y}_i \mid \boldsymbol{\eta}_i)$ , which in turn implies  $f(\boldsymbol{\eta}) = \sum_i f_i(\boldsymbol{\eta}_i)$ , where  $f_i$  is the logarithm of the marginal data density function in the  $i$ -th partition. In some cases, a proposal density based on the Gaussian approximation in (2.9) can be a poor approximation of the conditional posterior density in some partition of  $\boldsymbol{\eta}$ . Updating the whole vector  $\boldsymbol{\eta}$  in one block may then result in the MCMC chain getting stuck. As a result the computational efficiency of the sampler is reduced. In order to circumvent this issue and to retain the computational speed gained by using the Gaussian approximation in (2.9)

as a proposal density, a modification can be made to the sampling scheme which utilizes the conditional independence of the partitions within the data-rich block. The details on the modification can be seen in Appendix A. The resulting sampling scheme is outlined in Algorithm 1. Note that by choosing  $I = 1$  in Algorithm 1, the above sampling scheme without the conditional independence assumptions on the likelihood is obtained, while selecting  $I \geq 2$  in Algorithm 1 assumes the aforementioned partitioning of  $\boldsymbol{\eta}$  and that each  $\boldsymbol{\eta}_i$  is accepted or rejected separately.

---

**Algorithm 1** The proposed algorithm for obtaining the  $(k + 1)$ -th sample from  $\pi(\boldsymbol{\eta}|\mathbf{y}, \boldsymbol{\nu}, \boldsymbol{\theta})$  in the data-rich block. By choosing  $I = 1$ , the sampling scheme introduced in Section 2.3 is obtained. For  $I \geq 2$  the modified sampling scheme, which is derived in Appendix A, is obtained for the partitions.

---

**Input:**  $(\boldsymbol{\eta}^k, \boldsymbol{\nu}^k)$

- 1: Find the mode  $\boldsymbol{\eta}^0 = \arg \max_{\boldsymbol{\eta}} \log \pi(\boldsymbol{\eta}|\mathbf{y}, \boldsymbol{\nu}^k, \boldsymbol{\theta})$
- 2: Calculate  $\mathbf{H} = \nabla^2 f(\boldsymbol{\eta}^0)$  and  $\mathbf{b} = \nabla f(\boldsymbol{\eta}^0) - \mathbf{H}\boldsymbol{\eta}^0$
- 3: Sample  $\boldsymbol{\eta}^* \sim \mathcal{N}(\boldsymbol{\eta}^0, (\mathbf{Q}_\epsilon - \mathbf{H})^{-1})$
- 4: Calculate  $\boldsymbol{\rho}(\boldsymbol{\eta}^k)$  and  $\boldsymbol{\rho}(\boldsymbol{\eta}^*)$ , where

$$\boldsymbol{\rho}(\boldsymbol{\eta}) = \left( -\frac{1}{2} \boldsymbol{\eta}^\top \mathbf{H} - \mathbf{b}^\top \right) \circ \boldsymbol{\eta}$$

and  $\circ$  denotes an entrywise product

- 5: **for**  $i = 1, \dots, I$
- 6:   Calculate  $r_i = f_i(\boldsymbol{\eta}_i^*) + \boldsymbol{\rho}(\boldsymbol{\eta}^*)_i^\top \mathbf{1} - (f_i(\boldsymbol{\eta}_i^k) + \boldsymbol{\rho}(\boldsymbol{\eta}^k)_i^\top \mathbf{1})$
- 7:   Calculate  $\alpha_i = \min\{1, \exp r_i\}$
- 8:   Sample  $u_i \sim \mathcal{U}(0, 1)$
- 9:   **if**  $\alpha_i > u_i$
- 10:      $\boldsymbol{\eta}_i^{k+1} = \boldsymbol{\eta}_i^*$
- 11:   **else if**  $\alpha_i < u_i$
- 12:      $\boldsymbol{\eta}_i^{k+1} = \boldsymbol{\eta}_i^k$
- 13:   **end if**
- 14: **end for**

**Output:**  $\boldsymbol{\eta}^{k+1}$

---

## 2.4 Sampler for the data-poor block

The parameters  $(\boldsymbol{\nu}, \boldsymbol{\theta})$  in the data-poor block are, by construction, conditionally independent of  $\mathbf{y}$  conditioned on the vector  $\boldsymbol{\eta}$  from the data-rich block, that is,

$$\pi(\boldsymbol{\nu}, \boldsymbol{\theta} \mid \mathbf{y}, \boldsymbol{\eta}) = \pi(\boldsymbol{\nu}, \boldsymbol{\theta} \mid \boldsymbol{\eta}).$$

The conditional posterior density function of the data-poor block is therefore invariant of the choice of likelihood function and proportional to

$$\pi(\boldsymbol{\nu}, \boldsymbol{\theta} \mid \mathbf{y}, \boldsymbol{\eta}) \propto \pi(\boldsymbol{\nu} \mid \boldsymbol{\eta}, \boldsymbol{\theta})\pi(\boldsymbol{\theta}) \quad (2.12)$$

where the conditional density function  $\pi(\boldsymbol{\nu} \mid \boldsymbol{\eta}, \boldsymbol{\theta})$  is a Gaussian density of the form given in equation (2.6). Moreover, if the Gaussian density functions in the prior assumptions in (2.4) are GMRFs with sparse precision structures then the Gaussian density function in (2.6) retains the sparse GMRF structure induced by the prior assumption, by known results about conditioning of GRMFs [Rue and Held, 2005]. Fast sampling algorithms for GMRFs can thus be implemented to obtain samples from the Gaussian density function in (2.6), as discussed in Rue [2001].

The relation in (2.12) and the Gaussianity of  $\pi(\boldsymbol{\nu} \mid \boldsymbol{\eta}, \boldsymbol{\theta})$  in (2.6) motivate the following Metropolis–Hastings based sampling algorithm, which is a modified version of the one block sampler of Knorr-Held and Rue [2002]. For some proposal density  $q(\boldsymbol{\theta}^* \mid \boldsymbol{\theta}^k)$  for the hyperparameters  $\boldsymbol{\theta}$ , a new proposed value  $(\boldsymbol{\nu}^*, \boldsymbol{\theta}^*)$  is generated jointly as follows:

$$\begin{aligned} \boldsymbol{\theta}^* &\sim q(\boldsymbol{\theta}^* \mid \boldsymbol{\theta}^k) \\ \boldsymbol{\nu}^* &\sim \pi(\boldsymbol{\nu}^* \mid \boldsymbol{\eta}^{k+1}, \boldsymbol{\theta}^*). \end{aligned} \quad (2.13)$$

Denote the proposal density implied by (2.13) with  $q(\boldsymbol{\nu}^*, \boldsymbol{\theta}^* \mid \boldsymbol{\nu}^k, \boldsymbol{\theta}^k)$ . The proposed value  $(\boldsymbol{\nu}^*, \boldsymbol{\theta}^*)$  is then accepted jointly with acceptance probability

$$\alpha = \min \left\{ 1, \frac{\pi(\boldsymbol{\nu}^*, \boldsymbol{\theta}^* \mid \mathbf{y}, \boldsymbol{\eta}^{k+1}) q(\boldsymbol{\nu}^k, \boldsymbol{\theta}^k \mid \boldsymbol{\nu}^*, \boldsymbol{\theta}^*)}{\pi(\boldsymbol{\nu}^k, \boldsymbol{\theta}^k \mid \mathbf{y}, \boldsymbol{\eta}^{k+1}) q(\boldsymbol{\nu}^*, \boldsymbol{\theta}^* \mid \boldsymbol{\nu}^k, \boldsymbol{\theta}^k)} \right\}. \quad (2.14)$$

In Lemma 4 we show how the acceptance ratio in (2.14) can be simplified, which is modified version of the results shown in Knorr-Held and Rue [2002].

**Lemma 4.** *Assume the proposal density implied by (2.13) for the data-poor block, and denote the proposal density with  $q(\boldsymbol{\nu}^*, \boldsymbol{\theta}^* \mid \boldsymbol{\nu}^k, \boldsymbol{\theta}^k)$ . The corresponding acceptance ratio in (2.14), can be simplified to*

$$\frac{\pi(\boldsymbol{\nu}^*, \boldsymbol{\theta}^* \mid \mathbf{y}, \boldsymbol{\eta}^{k+1}) q(\boldsymbol{\nu}^k, \boldsymbol{\theta}^k \mid \boldsymbol{\nu}^*, \boldsymbol{\theta}^*)}{\pi(\boldsymbol{\nu}^k, \boldsymbol{\theta}^k \mid \mathbf{y}, \boldsymbol{\eta}^{k+1}) q(\boldsymbol{\nu}^*, \boldsymbol{\theta}^* \mid \boldsymbol{\nu}^k, \boldsymbol{\theta}^k)} = \frac{\pi(\boldsymbol{\theta}^* \mid \boldsymbol{\eta}^{k+1}) q(\boldsymbol{\theta}^k \mid \boldsymbol{\theta}^*)}{\pi(\boldsymbol{\theta}^k \mid \boldsymbol{\eta}^{k+1}) q(\boldsymbol{\theta}^* \mid \boldsymbol{\theta}^k)} \quad (2.15)$$

and is therefore independent of the value of  $\boldsymbol{\nu}$ .

In other words, the acceptance ratio in (2.15) is only dependent on the acceptance ratio for  $\boldsymbol{\theta}$ . Further, since the conditional posterior  $\pi(\boldsymbol{\nu} \mid \boldsymbol{\eta}, \boldsymbol{\theta})$  is a known Gaussian the proposed sampling strategy scales well in terms of computational efficiency as the dimensions of the data-poor component of the latent field  $\boldsymbol{\nu}$  increases.

When the Gaussian models in the prior assumptions (2.4) are GMRF density functions with a sparse precision structure, the ratio in (2.15) is computationally costly to calculate directly, since  $\pi(\boldsymbol{\theta} \mid \boldsymbol{\eta}) \propto \pi(\boldsymbol{\theta})\pi(\boldsymbol{\eta} \mid \boldsymbol{\theta})$  and  $\pi(\boldsymbol{\eta} \mid \boldsymbol{\theta})$  does not necessarily preserve the sparse GMRF structure. However, as the ratio in (2.15) is only dependent on the acceptance ratio for  $\boldsymbol{\theta}$  it can be shown that the ratio in (2.15) can be rewritten in order to preserve the sparse GMRF precision structure, as stated in the Theorem 5.

**Theorem 5.** *The term  $\pi(\boldsymbol{\theta}^* | \boldsymbol{\eta}^{k+1})/\pi(\boldsymbol{\theta}^k | \boldsymbol{\eta}^{k+1})$  in (2.15) can be rewritten as*

$$\frac{\pi(\boldsymbol{\theta}^* | \boldsymbol{\eta}^{k+1})}{\pi(\boldsymbol{\theta}^k | \boldsymbol{\eta}^{k+1})} = \frac{\pi(\boldsymbol{\theta}^*)}{\pi(\boldsymbol{\theta}^k)} \cdot \frac{\pi(\boldsymbol{\eta}^{k+1} | \mathbf{0}, \boldsymbol{\theta}^*)\pi(\mathbf{0} | \boldsymbol{\theta}^*)}{\pi(\mathbf{0} | \boldsymbol{\eta}^{k+1}, \boldsymbol{\theta}^*)} \cdot \frac{\pi(\mathbf{0} | \boldsymbol{\eta}^{k+1}, \boldsymbol{\theta}^k)}{\pi(\boldsymbol{\eta}^{k+1} | \mathbf{0}, \boldsymbol{\theta}^k)\pi(\mathbf{0} | \boldsymbol{\theta}^k)} \quad (2.16)$$

*Additionally, the conditional density functions on the right hand side in (2.16) on a logarithmic scale are*

$$\begin{aligned} \log \pi(\boldsymbol{\eta} | \mathbf{0}, \boldsymbol{\theta}) &= \frac{1}{2} \log \det \mathbf{Q}_\epsilon - \frac{1}{2} \boldsymbol{\eta}^\top \mathbf{Q}_\epsilon \boldsymbol{\eta} + \text{const} \\ \log \pi(\mathbf{0} | \boldsymbol{\theta}) &= \frac{1}{2} \log \det \mathbf{Q}_\nu + \text{const} \\ \log \pi(\mathbf{0} | \boldsymbol{\eta}, \boldsymbol{\theta}) &= \frac{1}{2} \log \det \left( \mathbf{Q}_\nu + \mathbf{Z}^\top \mathbf{Q}_\epsilon \mathbf{Z} \right) + \\ &\quad \left( \left( \mathbf{Q}_\nu + \mathbf{Z}^\top \mathbf{Q}_\epsilon \mathbf{Z} \right)^{-1} \mathbf{Z}^\top \mathbf{Q}_\epsilon \boldsymbol{\eta} \right) \mathbf{Z}^\top \mathbf{Q}_\epsilon \boldsymbol{\eta} + \text{const} \end{aligned} \quad (2.17)$$

*Moreover, if the Gaussian prior density functions in (2.4) are GMRFs with sparse precision structures, then all of the conditional density functions on the right hand side of (2.16) are GMRFs with sparse precision structures.*

Theorem 5 shows how the ratio in (2.14) can be calculated with low computational cost by using the results in (2.15), (2.16) and (2.17) in case of GMRFs with sparse precision structures. This is a key result for the implementation of the proposed sampling scheme in the data-poor block for GMRFs with sparse precision structures. The algorithm for the sampling scheme in the data-poor block is summarized in Algorithm 2.

### 3 Examples

Two examples are presented in this section where the MCMC split sampler is applied to obtain posterior samples from the proposed models. In the former example, a data set on annual mean precipitation in Iceland is modeled with a LGM that has a spatial model structure at the latent level. The latter example is on extreme flood events.

We will emphasize that the aim of this section is to present some of the possibilities offered by the MCMC split sampler rather than to claim which model is the best for each data set. The main purpose of the first example is to demonstrate that the MCMC split sampler is well suited to infer LGMs with a spatial models on both location and scale parameters of the data density function, and that the computational efficiency of the sampler scales well as the number of unobserved spatial grid points increases. The main goal of the latter example is show that the MCMC split sampler is designed to infer LGMs with a non-Gaussian three parameter data density function, where all the three parameters are modeled with latent Gaussian models.

---

**Algorithm 2** The proposed algorithm for obtaining the  $(k + 1)$ -th sample from  $\pi(\boldsymbol{\nu}, \boldsymbol{\theta} | \mathbf{y}, \boldsymbol{\eta})$  in the data-poor block.

---

**Input:**  $(\boldsymbol{\nu}^k, \boldsymbol{\theta}^k, \boldsymbol{\eta}^{k+1})$

- 1: Sample each element of  $\boldsymbol{\theta}^*$  from a proposal density  $q(\boldsymbol{\theta}^* | \boldsymbol{\theta}^k)$
- 2: Calculate

$$r = \frac{\pi(\boldsymbol{\theta}^*)}{\pi(\boldsymbol{\theta}^k)} \cdot \frac{\pi(\boldsymbol{\eta}^{k+1} | \mathbf{0}, \boldsymbol{\theta}^*) \pi(\mathbf{0} | \boldsymbol{\theta}^*)}{\pi(\mathbf{0} | \boldsymbol{\eta}^{k+1}, \boldsymbol{\theta}^*)} \frac{\pi(\mathbf{0} | \boldsymbol{\eta}^{k+1}, \boldsymbol{\theta}^k)}{\pi(\boldsymbol{\eta}^{k+1} | \mathbf{0}, \boldsymbol{\theta}^k) \pi(\mathbf{0} | \boldsymbol{\theta}^k)} \cdot \frac{q(\boldsymbol{\theta}^k | \boldsymbol{\theta}^*)}{q(\boldsymbol{\theta}^* | \boldsymbol{\theta}^k)}$$

on a logarithmic scale, using the equations in (2.17) for the conditional posterior densities functions

- 3: Calculate  $\alpha = \min \{1, r\}$
- 4: Sample  $u \sim \mathcal{U}(0, 1)$
- 5: **if**  $\alpha > u$
- 6:    Calcualte  $\mathbf{Q}_{\boldsymbol{\nu} | \boldsymbol{\eta}} = \mathbf{Q}_{\boldsymbol{\nu}} + \mathbf{Z}^\top \mathbf{Q}_\epsilon \mathbf{Z}$
- 7:    Sample  $\boldsymbol{\nu}^*$  from

$$\boldsymbol{\nu}^* | \boldsymbol{\eta}^{k+1}, \boldsymbol{\theta}^* \sim \mathcal{N} \left( \boldsymbol{\nu}^* \middle| \mathbf{Q}_{\boldsymbol{\nu} | \boldsymbol{\eta}}^{-1} (\mathbf{Q}_{\boldsymbol{\nu}} \boldsymbol{\mu}_{\boldsymbol{\nu}} + \mathbf{Z}^\top \mathbf{Q}_\epsilon \boldsymbol{\eta}^{k+1}), \mathbf{Q}_{\boldsymbol{\nu} | \boldsymbol{\eta}}^{-1} \right)$$

- 8:     $(\boldsymbol{\nu}^{k+1}, \boldsymbol{\theta}^{k+1}) = (\boldsymbol{\nu}^*, \boldsymbol{\theta}^*)$
  - 9: **else if**  $\alpha < u$
  - 10:     $(\boldsymbol{\nu}^{k+1}, \boldsymbol{\theta}^{k+1}) = (\boldsymbol{\nu}^k, \boldsymbol{\theta}^k)$
  - 11: **end if**
- Output:**  $(\boldsymbol{\nu}^{k+1}, \boldsymbol{\theta}^{k+1})$
-

### 3.1 Annual mean precipitation in Iceland

The data set analyzed in this section is on observations on annual precipitation from 86 observational sites across Iceland, see Figure 1, over the years 1962 to 2006. Times series on annual precipitation from the observational sites Reykjavík, Æðey, Akureyri and Kvísker are shown in Figure 2. The data was provided by the Icelandic Meteorological Office (IMO).

A LGM with a SPDE spatial model structure [Lindgren et al., 2011] at the latent level is presented to obtain the spatially varying distributional properties of annual precipitation over the domain. We will demonstrate that the computational efficiency of the MCMC split sampler scales well as the number of grid points in the mesh in the SPDE approach increase.

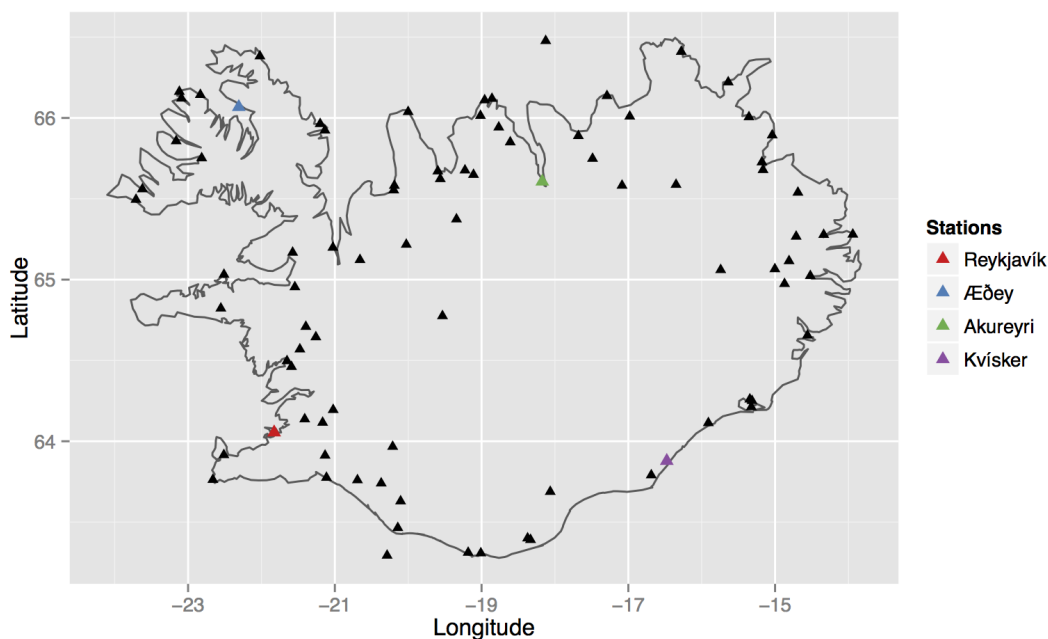


Figure 1: The  $I = 86$  observational sites in Iceland. Reykjavík is marked with red, Æðey is marked with blue, Akureyri is marked with green and Kvísker is marked with purple.

#### Model setup

**The data level:** The data were modeled with a LGM assuming the Gaussian distribution for the observations and conditional independence over the observational sites. That is, let  $y_{it}$  denote the annual precipitation at observational site  $i$  at year  $t$  then the

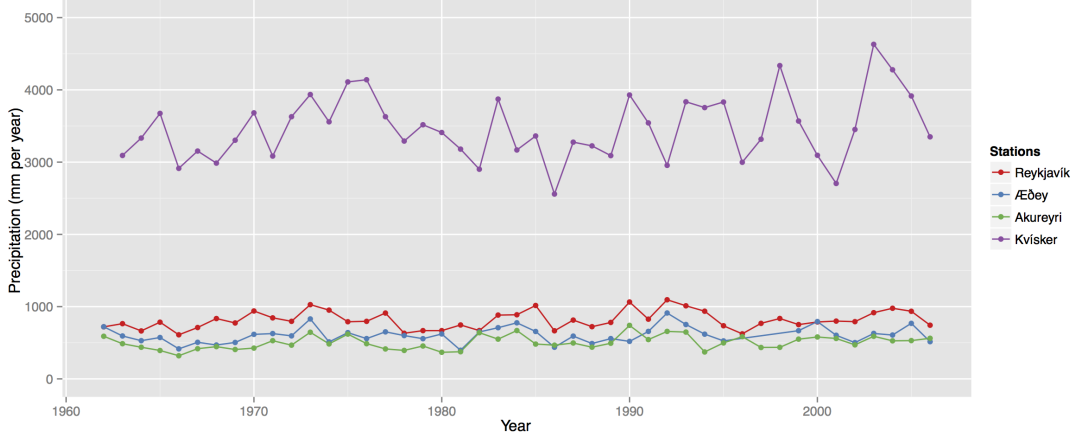


Figure 2: Times series over the years 1962 to 2006 on annual precipitation. The time series are based on observations from Reykjavík (red curve), Æðey (blue curve), Akureyri (green curve) and Kvísker (purple curve).

data density function becomes

$$\pi(y_{it} | \mu_i, \tau_i) = \mathcal{N}(y_{it} | \mu_i, \exp(\tau_i)), \quad i = 1, \dots, I, \quad t = 1, \dots, T$$

where  $I$  is the number of sites,  $T$  is the number of years;  $\mu_i$  and  $\tau_i$  are mean and log-variance parameters, respectively, which are both allowed to vary spatially.

**The latent level:** The following model structure was implemented for the mean parameter  $\boldsymbol{\mu} = (\mu_1, \dots, \mu_I)$  at the latent level of the model,

$$\boldsymbol{\mu} = \mathbf{X}_\mu \boldsymbol{\beta}_\mu + \mathbf{A}_\mu \mathbf{u}_\mu + \boldsymbol{\epsilon}_\mu,$$

where  $\mathbf{X}_\mu$  is a design matrix consisting of a vector of ones and covariates that are based on the meteorological model of Crochet et al. [2007], see Geirsson et al. [2015] for details;  $\boldsymbol{\beta}_\mu$  are the corresponding weights;  $\mathbf{u}_\mu$  denotes a Matérn type spatial field constructed with the SPDE approach [Lindgren et al., 2011] on a triangulated mesh over the spatial domain with a smoothness parameters chosen as one, which corresponds to an almost once differentiable Matérn field and  $\alpha = 2$  in the SPDE method;  $\mathbf{A}_\mu$  is a known projection matrix; the matrix product  $\mathbf{A}_\mu \mathbf{u}_\mu$  then denotes the spatial effect at the observational sites, which captures the spatial variation in the data that is unexplained by the covariate and  $\boldsymbol{\epsilon}_\mu$  is an unstructured random effect. Analogous model structure is also implemented for the log-variance parameter, that is

$$\boldsymbol{\tau} = \mathbf{X}_\tau \boldsymbol{\beta}_\tau + \mathbf{A}_\tau \mathbf{u}_\tau + \boldsymbol{\epsilon}_\tau.$$

where  $\mathbf{X}_\tau$  is a design matrix consisting of a vector of ones and the aforementioned meteorological covariate on a logarithmic scale.

Working within the LGM setup, the following prior density functions were assigned to parameters at the latent level of the model.

$$\begin{aligned}\pi(\boldsymbol{\beta}_\mu) &= \mathcal{N}(\boldsymbol{\beta}_\mu \mid \mathbf{0}, \kappa_{\beta\mu}^{-1}\mathbf{I}), & \pi(\boldsymbol{\beta}_\tau) &= \mathcal{N}(\boldsymbol{\beta}_\tau \mid \mathbf{0}, \kappa_{\beta\tau}^{-1}\mathbf{I}), \\ \pi(\mathbf{u}_\mu) &= \mathcal{N}(\mathbf{u}_\mu \mid \mathbf{0}, \mathbf{Q}_{u\mu}^{-1}), & \pi(\mathbf{u}_\tau) &= \mathcal{N}(\mathbf{u}_\tau \mid \mathbf{0}, \mathbf{Q}_{u\tau}^{-1}), \\ \pi(\boldsymbol{\epsilon}_\mu) &= \mathcal{N}(\boldsymbol{\epsilon}_\mu \mid \mathbf{0}, \sigma_{\epsilon\mu}^2\mathbf{I}), & \pi(\boldsymbol{\epsilon}_\tau) &= \mathcal{N}(\boldsymbol{\epsilon}_\tau \mid \mathbf{0}, \sigma_{\epsilon\tau}^2\mathbf{I}).\end{aligned}$$

The parameter values  $\kappa_{\beta\mu} = 0.0025$  and  $\kappa_{\beta\tau} = 0.25$  were fixed in the prior distributions for  $\boldsymbol{\beta}_\mu$  and  $\boldsymbol{\beta}_\tau$ . The precision matrices  $\mathbf{Q}_{u\mu}$  and  $\mathbf{Q}_{u\tau}$  are constructed with SPDE approach, and have sparse GMRF precision structures. Further, the precision matrix  $\mathbf{Q}_{u\mu}$  has two parameters,  $\sigma_{u\mu}$  and  $\kappa_{u\mu}$ , which serve as hyperparameters of the spatial model for  $\mu$ . The hyperparameters  $\sigma_{u\mu}$  and  $\kappa_{u\mu}$  are related to the marginal variance and range of the spatial field, respectively. Analogous structure holds for  $\mathbf{Q}_{u\tau}$ . The parameters  $\sigma_{\epsilon\mu}^2$  and  $\sigma_{\epsilon\tau}^2$  are unknown variance parameters for the unstructured random effects.

**The hyper level:** Let  $\boldsymbol{\theta}$  denote all the hyper parameters of the model that are not fixed, that is

$$\boldsymbol{\theta} = (\sigma_{u\mu}, \kappa_{u\mu}, \sigma_{\epsilon\mu}, \sigma_{u\tau}, \kappa_{u\tau}, \sigma_{\epsilon\tau}).$$

Lognormal prior distributions with fixed parameters were assigned to the hyperparameters in  $\boldsymbol{\theta}$ .

### Posterior inference

In order to apply the MCMC split sampler to the aforementioned model, the model parameters are assigned to the data-rich block which includes  $\boldsymbol{\eta} = (\boldsymbol{\mu}, \boldsymbol{\tau})$  and the data-poor block which consists of  $\boldsymbol{\nu} = (\boldsymbol{\beta}_\mu, \mathbf{u}_\mu, \boldsymbol{\beta}_\tau, \mathbf{u}_\tau)$  and the hyperparameters  $\boldsymbol{\theta}$ .

The aforementioned model setup and prior assumptions are equivalent to the setup implied in equations (2.3) and (2.4) with

$$\begin{aligned}\mathbf{Z} &= \begin{pmatrix} \mathbf{X}_\mu & \mathbf{A}_\mu & \cdot & \cdot \\ \cdot & \cdot & \mathbf{X}_\tau & \mathbf{A}_\tau \end{pmatrix}, & \mathbf{Q}_\epsilon &= \begin{pmatrix} \sigma_{\epsilon\mu}^{-2}\mathbf{I} & \cdot \\ \cdot & \sigma_{\epsilon\tau}^{-2}\mathbf{I} \end{pmatrix} \\ \mathbf{Q}_\nu &= \begin{pmatrix} \kappa_{\beta\mu}\mathbf{I} & \cdot & \cdot & \cdot \\ \cdot & \mathbf{Q}_{u\mu} & \cdot & \cdot \\ \cdot & \cdot & \kappa_{\beta\tau}\mathbf{I} & \cdot \\ \cdot & \cdot & \cdot & \mathbf{Q}_{u\tau} \end{pmatrix}.\end{aligned}\tag{3.1}$$

**Data-rich block:** The conditional posterior  $\pi(\boldsymbol{\eta} \mid \mathbf{y}, \boldsymbol{\nu}, \boldsymbol{\theta})$  in the data-rich block is intractable. However, the logarithm of the conditional posterior of the data-rich block is of the same form as in equation (2.8), with  $\mathbf{Z}$  and  $\mathbf{Q}_\epsilon$  defined in equation (3.1) and

$$f(\boldsymbol{\eta}) = \sum_{i=1}^I f_i(\boldsymbol{\eta}_i) = \sum_{i=1}^I \sum_{t \in \mathcal{A}_i} \log \mathcal{N}(y_{it} \mid \mu_i, \exp \tau_i),\tag{3.2}$$

where the set  $\mathcal{A}_i$  contains the indices of the years  $t$  observed at site  $i$ . By model assumptions, the vectors  $\boldsymbol{\eta}_i = (\mu_i, \tau_i)$  become conditionally independent in the conditional posterior  $\pi(\boldsymbol{\eta} \mid \mathbf{y}, \boldsymbol{\nu}, \boldsymbol{\theta})$  over observational sites  $i$ . This demonstrates that the modification of the sampling scheme in Section 2.3, outlined in Appendix A, is applicable. Therefore Algorithm 1 was used to obtain MCMC samples from the conditional posterior  $\pi(\boldsymbol{\eta} \mid \mathbf{y}, \boldsymbol{\nu}, \boldsymbol{\theta})$  with  $I = 86$ ,  $\mathbf{Q}_\epsilon$  as in (3.1) and  $f(\boldsymbol{\eta})$  as in (3.2).

**Data-poor block:** In order to implement the sampling strategy outlined in Section 2.4 and to obtain MCMC samples from the conditional posterior  $\pi(\boldsymbol{\nu}, \boldsymbol{\theta} \mid \mathbf{y}, \boldsymbol{\eta})$ , a proposal density  $q$  for the hyperparameters  $\boldsymbol{\theta}$  must be chosen. In this example, the proposal strategy suggested in [Knorr-Held and Rue, 2002] is used for each element of  $\boldsymbol{\theta}$ . That is, let  $\theta_i^* = f\theta_i^k$  where the scaling factor  $f$  has the density

$$\pi(f) \propto 1 + 1/f \quad \text{for } f \in [1/F, F] \quad (3.3)$$

where  $F > 1$  is a tuning parameter. Knorr-Held and Rue [2002] show that this is a symmetric proposal density in the sense that  $q(\theta_i^* \mid \theta_i^k) = q(\theta_i^k \mid \theta_i^*)$ . Therefore, by using this proposal density, the acceptance probability in equation (2.14) simplifies to

$$\alpha = \min \left\{ 1, \frac{\pi(\boldsymbol{\theta}^* \mid \boldsymbol{\eta}^{k+1})}{\pi(\boldsymbol{\theta}^k \mid \boldsymbol{\eta}^{k+1})} \right\}$$

Moreover, the ratio in (2.16) in Theorem 5 was used to calculate the acceptance probability, which preserves the sparse GMRF precision structure induced by the SPDE approach. Thus, Algorithm 2 is was implemented to obtain MCMC samples from the conditional posterior  $\pi(\boldsymbol{\eta} \mid \mathbf{y}, \boldsymbol{\nu}, \boldsymbol{\theta})$ , with  $\mathbf{Z}$ ,  $\mathbf{Q}_\epsilon$  and  $\mathbf{Q}_\nu$  defined in (3.1) and the proposal density in (3.3).

### Convergence diagnostics

The following convergence diagnostics are based on four MCMC chains sampled in parallel with the MCMC split sampler from the proposed model. Each chain was calculated with 50000 iterations where 10000 iterations were burned in. The posterior inference was carried out separately for three different mesh resolutions. That is, a coarse resolution based on 411 mesh points; a medium resolution based on 858 mesh points; and a dense resolution based 1752 mesh points. In Figure 3 the three different meshes are presented on a same scale. The top, middle and bottom panels in Figure 3 show the coarse resolution, medium resolution and dense resolution meshes, respectively. Runtime, on a modern desktop (Ivy Bridge Intel Core i7-3770K, 16GB RAM and a solid state hard drive), was approximately 6, 6.5 and 7 hours for the coarse, medium and dense mesh resolution, respectively. All calculations were carried out using R.

Gelman–Rubin plots, based on the MCMC runs, of the the mean parameter  $\mu$  in Reykjavík; the covariate coefficient  $\beta_{\mu 2}$ ; and the marginal standard deviation for the spatial field  $\sigma_{u\mu}$  are shown in the first, second and third column, respectively, in Figure

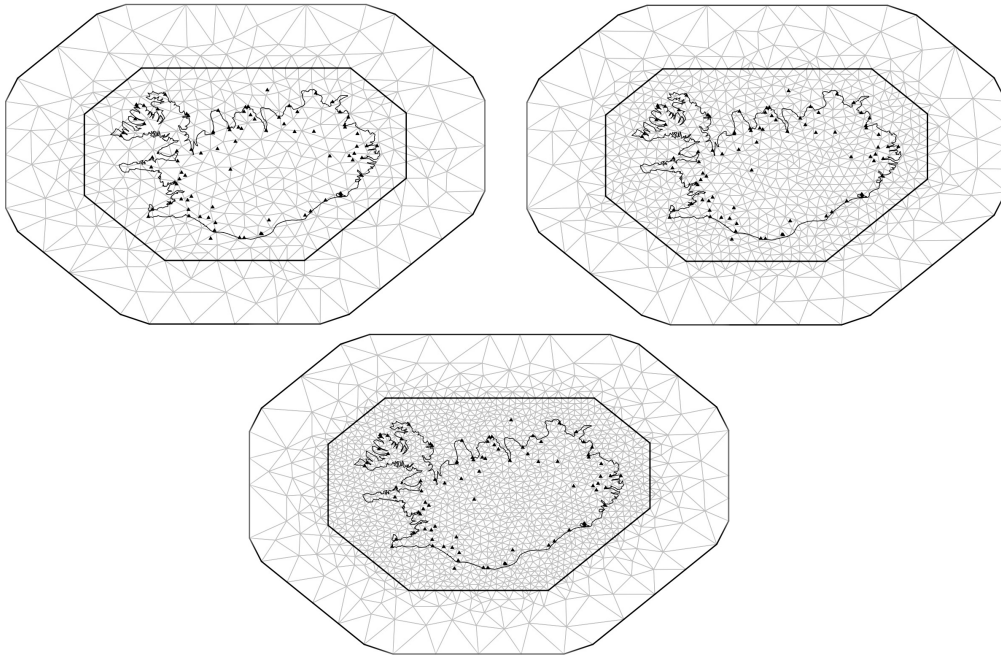


Figure 3: The triangulated meshes over the spatial domain, based on the coarse mesh (top left), medium mesh (top right) and dense mesh (bottom).

4. The results based on the coarse resolution, medium resolution and dense resolution meshes for the aforementioned parameters are shown in the first, second and third row, respectively, in Figure 4. A comparison of the results in Figure 4 between the different mesh resolutions reveals that the convergence in the mean is achieved for the three parameters at a similar rate. Furthermore, the Gelman–Rubin plots in Figure 4 show that the sampler has converged in the mean after roughly 7500 iterations for all mesh resolutions. Similar results hold for all of the other model parameters (results not shown).

Autocorrelation plots for the same set of parameters and arranged identically as in Figure 4 are shown in Figure 5. The results demonstrate that the MCMC chains for the mean parameter  $\mu$  in Reykjavik and the covariate coefficient  $\beta_{\mu 2}$  exhibit a negligible autocorrelation after lag 10. The MCMC samples of the hyperparameter  $\sigma_{u\mu}$  show autocorrelation around 0.3 at lag 50. Similar results hold for all the other model parameters (results not shown).

Relying on the Gelman-Rubin statistics and the autocorrelation plots, the MCMC chains exhibit all signs of having converged. Moreover, the autocorrelation plots in Figure 5 reveal that the autocorrelation in the MCMC chains does not increase with number of mesh points, which in turn indicates that the autocorrelation in the MCMC chains is invariant of the dimensions of the data-poor part of the latent field  $\boldsymbol{\nu}$ . These results demonstrate that the MCMC split sampler retains its computational efficiency when the number of mesh points increases, which is to be expected as the acceptance probability in (2.15) in the data-poor block is independent of the  $\boldsymbol{\nu}$ .

Furthermore, as the acceptance probability in (2.15) within the data-poor block is only dependent on the hyperparameters, the autocorrelation seen in MCMC chains for the hyperparameter  $\sigma_{u\mu}$  in Figure 5 is mainly affected by the choice of proposal density for  $\theta$ , which is in this example the sampler in (3.3). In Section 3.2 we will demonstrate the modularity of the MCMC split sampler, by choosing another proposal density for the hyperparameters  $\theta$  in Algorithm 2 which significantly reduces the autocorrelation in MCMC chains for  $\theta$ .

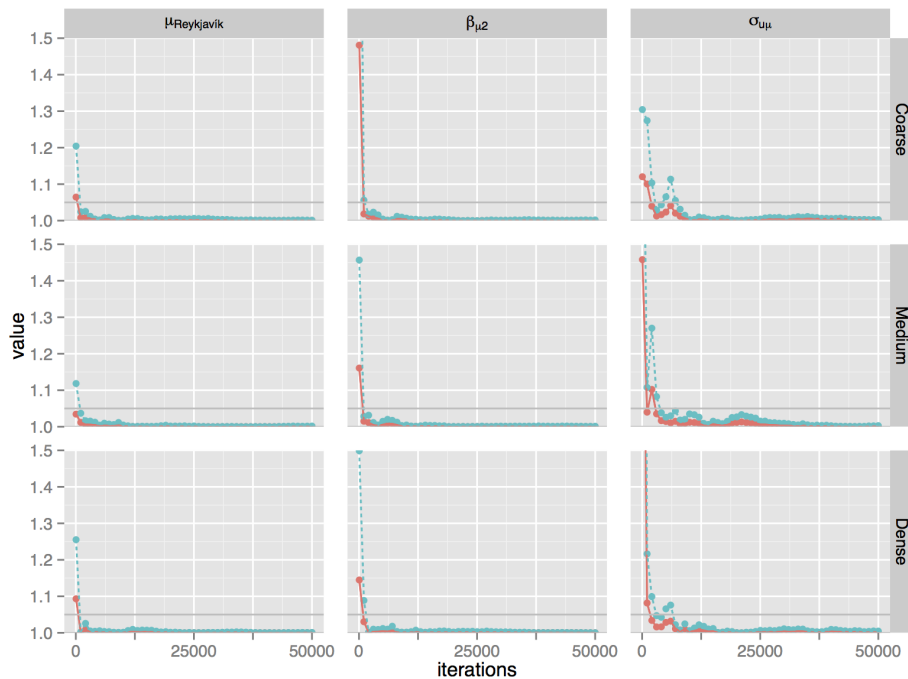


Figure 4: Gelman–Rubin plots for  $\mu$ ,  $\beta_{\mu 2}$ , and  $\sigma_{u\mu}$  for three different mesh resolutions. The red solid line denotes the median of the Gelman–Rubin statistics, and the green dashed line denoted the upper limit of the 95% confidence interval for the Gelman–Rubin statistics. The first row is based on a coarse resolution (411 mesh points). The second row is based on a medium resolution (858 mesh points). The third row is based on a dense resolution (1752 mesh points). The results demonstrate the MCMC split sampler has converged in the mean after roughly 7500 iterations.

### 3.2 Flood analysis

In this section, we present a simulation study on extreme events. The data set consists of simulations of monthly maximum instantaneous flow based on characteristics of ten river catchments around Iceland. The characterizing features that were used to simulate the data for each river were chosen as river catchment area and maximum daily precipitation, as both river catchment area and maximum daily precipitation are known to be positively

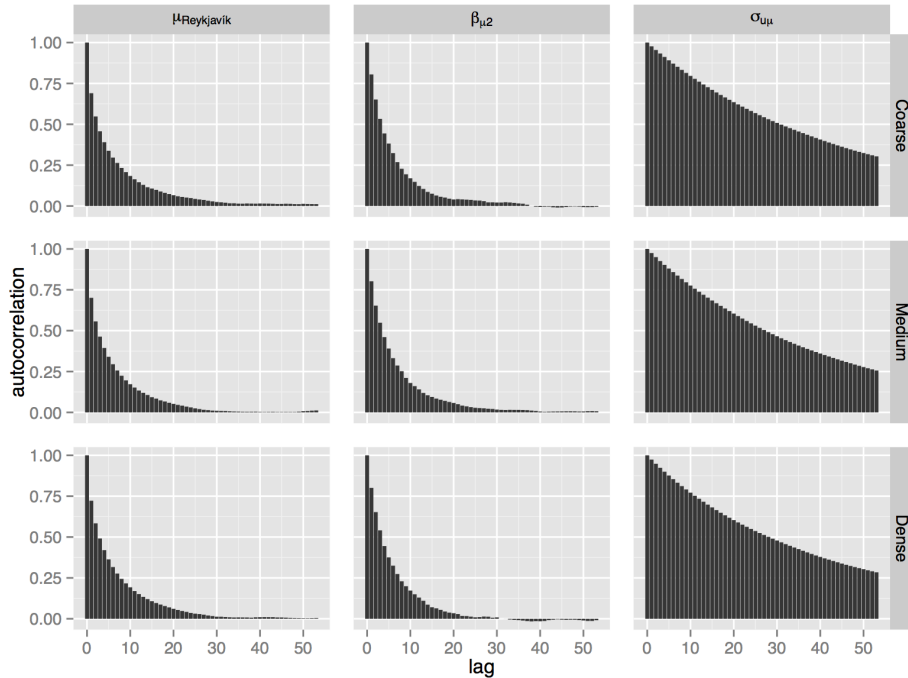


Figure 5: Autocorrelation plots for  $\mu$ ,  $\beta_{\mu 2}$ , and  $\sigma_{u\mu}$  for three different mesh sizes. The first row is based on a coarse resolution (411 mesh points). The second row is based on a medium resolution (858 mesh points). The third row is based on a dense resolution (1752 mesh points). The results demonstrate that the autocorrelation in the MCMC chains decays rapidly and is invariant of the number of points in the mesh.

correlated with maximum instantaneous flow, see Davíðsson [2015] and Crochet et al. [2012]. The simulated time series were chosen to be 150 years.

### Model setup

**The data level:** The data were modeled with a LGM assuming the generalized extreme value distribution (g.e.v.) for the observations. To that extend, let  $y_{mj,t}$  denote the value from river  $j$  at month  $m$  and year  $t$ , with a cumulative density function of the form

$$F(y_{mj,t}) = \exp \left\{ - \left( 1 + \xi_{mj} \left( \frac{y_{mj,t} - \mu_{mj}}{\sigma_{mj}} \right) \right)^{-1/\xi_{mj}} \right\}$$

if  $1 + \xi_{mj}(x - \mu_{mj})/\sigma_i > 0$ ,  $F(y_{it}) = 0$  otherwise. The parameters  $\mu_{mj}$ ,  $\sigma_{mj}$  and  $\xi_{mj}$  are the location, scale and shape parameters of the g.e.v. distribution for river  $j$  in month  $m$ . Additionally,  $J$  is the number of rivers and  $T$  is the number of years. Further, the data is assumed independent between both rivers and between months. These assumptions were made for demonstrative purposes.

**The latent level:** The location and scale parameters are modeled on a logarithmic scale at the latent level, which is modelling setup along the lines presented in Cunnane and Nash [1971] and GREHY [1996]. Thus, define  $\lambda_{mj} = \log \mu_{mj}$  and  $\tau_{mj} = \log \sigma_{mj}$ . The shape parameter is modeled on its native scale.

As discussed in Davíðsson [2015], the underlying processes of monthly maximum instantaneous flow exhibit a seasonal behavior. Therefore, the following seasonal model is proposed for the location parameter on a logarithmic scale. That is,

$$\begin{aligned} \lambda_{mj} = & \beta_{0,\lambda} + u_{0,m,\lambda} + x_{1,mj}(\beta_{1,\lambda} + u_{1,m,\lambda}) \\ & + \dots + x_{p,m,j}(\beta_{p,\lambda} + u_{p,m,\lambda}) + \epsilon_{mj,\lambda} \end{aligned} \quad (3.4)$$

where  $\beta_{0,\lambda}$  denotes an overall intercept term;  $x_{i,mj}$  denotes the  $i$ -th covariate in month  $m$  at the  $j$ -th river;  $\beta_{i,\lambda}$  denotes the weight of the  $i$ -th covariate for  $i = 1, \dots, p$ ;  $u_{0,m,\lambda}$  denotes the seasonal random effect of the  $m$ -th month;  $u_{i,m,\lambda}$  denotes the seasonal additional weight of the  $i$ -th covariate within month  $m$ ; and  $\epsilon_{mj,\lambda}$  denotes an unstructured random effect.

In order to write the model in a matrix form for the implementation of the MCMC split sampler, combine the location parameters for river  $j$  over months. That is,

$$\boldsymbol{\lambda}_j = (\lambda_{1j}, \dots, \lambda_{12j})^\top, \quad j = 1, \dots, J$$

and define the following

$$\mathbf{u}_{i,\lambda} = (u_{i,1,\lambda}, \dots, u_{i,12,\lambda})^\top, \mathbf{A}_{i,j} = \text{diag}(x_{i,j1}, \dots, x_{i,j12}),$$

where  $i = 0, \dots, p$  and  $x_{0,jm} = 1$  denotes the intercept term for river  $j$  and month  $m$ . Additionally, define

$$\mathbf{X}_j = \begin{pmatrix} 1 & x_{1,j,1} & \dots & x_{p,j,1} \\ 1 & x_{1,j,2} & \dots & x_{p,j,2} \\ \vdots & & \ddots & \\ 1 & x_{1,j,12} & \dots & x_{p,j,12} \end{pmatrix}, \quad \mathbf{A}_j = (\mathbf{A}_{0,j}, \dots, \mathbf{A}_{p,j}).$$

The seasonal model presented in (3.4) for the log-location parameter for river  $j$  can be written in matrix form as

$$\boldsymbol{\lambda}_j = \mathbf{X}_j \boldsymbol{\beta}_\lambda + \mathbf{A}_j \mathbf{u}_\lambda + \boldsymbol{\epsilon}_{j,\lambda}$$

where  $\boldsymbol{\beta}_\lambda = (\beta_{0,\lambda}, \dots, \beta_{p,\lambda})^\top$ ,  $\mathbf{u}_\lambda = (\mathbf{u}_{0,\lambda}, \dots, \mathbf{u}_{p,\lambda})^\top$ , and  $\boldsymbol{\epsilon}_{j,\lambda} = (\epsilon_{1j,\lambda}, \dots, \epsilon_{12j,\lambda})$ . By combing the seasonal model over rivers, the following holds

$$\boldsymbol{\lambda} = \mathbf{X} \boldsymbol{\beta}_\lambda + \mathbf{A} \mathbf{u}_\lambda + \boldsymbol{\epsilon}_\lambda$$

where

$$\boldsymbol{\lambda} = \begin{pmatrix} \boldsymbol{\lambda}_1 \\ \vdots \\ \boldsymbol{\lambda}_J \end{pmatrix}, \mathbf{X} = \begin{pmatrix} \mathbf{X}_1 \\ \vdots \\ \mathbf{X}_J \end{pmatrix}, \mathbf{A} = \begin{pmatrix} \mathbf{A}_1 \\ \vdots \\ \mathbf{A}_J \end{pmatrix}, \boldsymbol{\epsilon}_\lambda = \begin{pmatrix} \boldsymbol{\epsilon}_{1,\lambda} \\ \vdots \\ \boldsymbol{\epsilon}_{J,\lambda} \end{pmatrix}.$$

Analogous model structure was also implemented for the log-scale parameter. That is,

$$\boldsymbol{\tau} = \mathbf{X}\boldsymbol{\beta}_\tau + \mathbf{A}\mathbf{u}_\tau + \boldsymbol{\epsilon}_\tau.$$

A reduced model with a similar structure was implemented for the shape parameter  $\xi$ . That is

$$\xi_{mj} = \beta_{0,\xi} + u_{0,m,\xi} + \epsilon_{mj,\xi} \quad (3.5)$$

where  $\beta_{0,\xi}$  denotes an overall intercept term;  $u_{0,m,\xi}$  denotes the seasonal random effect of the  $m$ -th month; and  $\epsilon_{mj,\xi}$  denotes an unstructured random effect. The full matrix model for  $\xi$  becomes

$$\boldsymbol{\xi} = \mathbf{1}_{12J}\beta_{0,\xi} + (\mathbf{1}_J \otimes \mathbf{I}_{12})\mathbf{u}_\xi + \boldsymbol{\epsilon}_\xi$$

where  $\mathbf{1}_n$  denoted an  $n$ -dimensional vector of ones.

Working within the LGM framework, the following prior density functions were assigned to the latent parameters. First assign,

$$\pi(\boldsymbol{\beta}_\lambda) = \mathcal{N}(\boldsymbol{\beta}_\lambda \mid \mathbf{0}, \sigma_{\beta\lambda}^2 \mathbf{I}), \quad \pi(\boldsymbol{\beta}_\tau) = \mathcal{N}(\boldsymbol{\beta}_\tau \mid \mathbf{0}, \sigma_{\beta\tau}^2 \mathbf{I}) \quad \pi(\beta_\xi) = \mathcal{N}(\beta_\xi \mid 0, \sigma_{\beta\xi}^2).$$

The parameters  $\boldsymbol{\beta}_\lambda, \boldsymbol{\beta}_\tau$  and  $\beta_\xi$  are assumed *a priori* to have a low precision on their native scales in order to let the data play the dominate role in their inference. Thus, the parameter values  $\sigma_{\beta\lambda} = 4$ ,  $\sigma_{\beta\tau} = 4$  and  $\sigma_{\beta\xi} = 2$  were chosen for the prior density functions.

Secondly, the selection of prior density functions for the seasonal random effects needs to incorporate a correlation structure that induces a strong correlation between neighbouring months. This is achieved by assigning the following prior density functions

$$\begin{aligned} \pi(\mathbf{u}_\lambda) &= \mathcal{N}(\mathbf{u}_\lambda \mid \mathbf{0}, \text{diag}(\boldsymbol{\psi}_\lambda) \otimes \mathbf{Q}_u^{-1}), \\ \pi(\mathbf{u}_\tau) &= \mathcal{N}(\mathbf{u}_\tau \mid \mathbf{0}, \text{diag}(\boldsymbol{\psi}_\tau) \otimes \mathbf{Q}_u^{-1}), \\ \pi(\mathbf{u}_\xi) &= \mathcal{N}(\mathbf{u}_\xi \mid \mathbf{0}, \boldsymbol{\psi}_\xi \mathbf{Q}_u^{-1}) \end{aligned}$$

where  $\boldsymbol{\psi}_\lambda = (\psi_{0,\lambda}, \dots, \psi_{p,\lambda})^\top$ ,  $\boldsymbol{\psi}_\tau = (\psi_{0,\tau}, \dots, \psi_{p,\tau})^\top$  and  $\boldsymbol{\psi}_\xi$  serve as scaling parameters for the monthly random effects corresponding to the three intercepts and the covariates; and the  $\mathbf{Q}_u(\kappa)$  is a  $12 \times 12$  circular band precision matrix that has the vector

$$[1 \quad -2(\kappa^2 + 2) \quad \kappa^4 + 4\kappa^2 + 6 \quad -2(\kappa^2 + 2) \quad 1]$$

on the diagonal band, as discussed in Lindgren et al. [2011], which capture the autocorrelation between months. In this example, the decay parameters was fixed to simplify the inference and set equal to  $\kappa = 1$ . Further, this value of  $\kappa$  induces an autocorrelation *a priori* between consecutive months. Third, for the unstructured random effects, the following priors were chosen.

$$\pi(\boldsymbol{\epsilon}_\lambda) = \mathcal{N}(\boldsymbol{\epsilon}_\lambda \mid \mathbf{0}, \sigma_{\epsilon\lambda}^2 \mathbf{I}), \quad \pi(\boldsymbol{\epsilon}_\tau) = \mathcal{N}(\boldsymbol{\epsilon}_\tau \mid \mathbf{0}, \sigma_{\epsilon\tau}^2 \mathbf{I}), \quad \pi(\boldsymbol{\epsilon}_\xi) = \mathcal{N}(\boldsymbol{\epsilon}_\xi \mid \mathbf{0}, \sigma_{\epsilon\xi}^2 \mathbf{I}).$$

**The hyper level:** Let  $\boldsymbol{\theta}$  denote all the hyperparameters of the model that are not fixed on a logarithmic scale for computational purposes. That is,

$$\boldsymbol{\theta} = (\log \psi_{0,\lambda}, \dots, \log \psi_{p,\lambda}, \log \psi_{0,\tau}, \dots, \log \psi_{p,\tau}, \log \psi_\xi, \log \sigma_{\epsilon\lambda}^2, \log \sigma_{\epsilon\tau}^2, \log \sigma_{\epsilon\xi}^2)$$

Gaussian prior distributions with fixed parameters were assigned to the hyperparameters in  $\boldsymbol{\theta}$ .

### Posterior inference

The data-rich block includes  $\boldsymbol{\eta} = (\boldsymbol{\mu}, \boldsymbol{\tau}, \boldsymbol{\xi})$  and the data-poor block consists of  $\boldsymbol{\nu} = (\boldsymbol{\beta}_\mu, \mathbf{u}_\mu, \boldsymbol{\beta}_\tau, \mathbf{u}_\tau, \beta_\xi, \mathbf{u}_\xi)$  and the hyperparameters  $\boldsymbol{\theta}$ . For the implementations of the MCMC split sampler, define the following sparse matrices

$$\mathbf{Z} = \begin{pmatrix} \mathbf{X} & \mathbf{A} & \cdot & \cdot & \cdot & \cdot \\ \cdot & \cdot & \mathbf{X} & \mathbf{A} & \cdot & \cdot \\ \cdot & \cdot & \cdot & \cdot & \mathbf{1}_{12J} & \mathbf{I}_{12J} \end{pmatrix}, \mathbf{Q}_\epsilon = \begin{pmatrix} \sigma_{\epsilon\lambda}^{-2} \mathbf{I} & \cdot & \cdot \\ \cdot & \sigma_{\epsilon\tau}^{-2} \mathbf{I} & \cdot \\ \cdot & \cdot & \sigma_{\epsilon\xi}^{-2} \mathbf{I} \end{pmatrix} \quad (3.6)$$

and

$$\mathbf{Q}_\nu = \text{bdiag}(\sigma_{\beta\lambda}^{-2} \mathbf{I}, \text{diag}(\boldsymbol{\psi}_\lambda) \otimes \mathbf{Q}_u^{-1}, \sigma_{\beta\tau}^{-2} \mathbf{I}, \text{diag}(\boldsymbol{\psi}_\tau) \otimes \mathbf{Q}_u^{-1}, \sigma_{\beta\xi}^{-2}, \boldsymbol{\psi}_\xi \mathbf{Q}_u^{-1}) \quad (3.7)$$

where  $\text{bdiag}$  denotes a block diagonal matrix.

**Data-rich block:** The modified version of the sampling scheme in Section 2.3, outlined in Appendix A, was used to obtain MCMC samples from the conditional posterior  $\pi(\boldsymbol{\eta} \mid \mathbf{y}, \boldsymbol{\nu}, \boldsymbol{\theta})$ . The logarithm of the conditional posterior is of the same form as in equation (2.8), with  $\mathbf{Z}$  and  $\mathbf{Q}_\epsilon$  defined in equation (3.6) and

$$f(\boldsymbol{\eta}) = \sum_{m=1}^{12} \sum_{j=1}^J f_i(\boldsymbol{\eta}_{mj}) = \sum_{m=1}^{12} \sum_{j=1}^J \sum_{t=1}^T \log \pi_{\text{gev}}(y_{mj,t} \mid \exp \lambda_{mj}, \exp \tau_{mj}, \xi_{mj}) \quad (3.8)$$

where  $\pi_{\text{gev}}$  denotes the density function of the generalized extreme value distribution. Therefore, Algorithm 1 was used to obtain MCMC samples from the conditional posterior from the data-rich block, with  $I = J \cdot 12 = 120$ ,  $\mathbf{Q}_\epsilon$  as in (3.6) and  $f(\boldsymbol{\eta})$  as in (3.8).

**Data-poor block:** The sampling scheme outlined in Section 2.4 was used to obtain MCMC samples from the conditional posterior  $\pi(\boldsymbol{\nu}, \boldsymbol{\theta} \mid \mathbf{y}, \boldsymbol{\eta})$  in the data-poor block. A proposal density based on the normal distribution centered on the last draw of  $\boldsymbol{\theta}$ , as discussed in Roberts et al. [1997], was selected for Algorithm 2, with a precision matrix  $-c\mathbf{H}$  where  $\mathbf{H}$  is a finite difference estimate of the Hessian matrix of  $\log \pi(\boldsymbol{\theta} \mid \hat{\boldsymbol{\eta}})$  evaluated at the mode. That is,

$$\mathbf{H} \approx \nabla^2 \log \pi(\boldsymbol{\theta} \mid \hat{\boldsymbol{\eta}}) \Big|_{\boldsymbol{\theta}=\boldsymbol{\theta}_0} \quad (3.9)$$

where  $\hat{\boldsymbol{\eta}}$  is the maximum likelihood estimate of  $\boldsymbol{\eta}$  for each river and month;  $\boldsymbol{\theta}_0$  is the mode of  $\log \pi(\log \boldsymbol{\theta} | \hat{\boldsymbol{\eta}})$ ; and  $c$  is a scaling constant. Conditioning on  $\hat{\boldsymbol{\eta}}$ , as opposed of  $\boldsymbol{\eta}^{k+1}$  for example, removes the necessity to estimate  $\mathbf{H}$  in every iteration. Moreover, setting a specific scaling  $u$  removes the need for tuning. The scaling  $c = 2.382/\dim(\boldsymbol{\theta})$  was implemented, as it is optimal in a particular large dimension scenario, see Roberts et al. [1997]. The resulting proposal density therefore becomes

$$q(\boldsymbol{\theta}^* | \boldsymbol{\theta}^k) = \mathcal{N}\left(\boldsymbol{\theta}^* \mid \boldsymbol{\theta}^k, (-c\mathbf{H})^{-1}\right). \quad (3.10)$$

Algorithm 2 was thus implemented to obtain MCMC sampled from the conditional posterior within the data-poor block, with  $\mathbf{Z}$ ,  $\mathbf{Q}_\epsilon$  as in equation (3.6);  $\mathbf{Q}_\nu$  as in equation (3.7); and the proposal density in (3.10).

### Convergence diagnostics

As in Section 3.1, the following convergence diagnostics are based on four MCMC chains sampled in parallel with the MCMC split sampler. Each chain was calculated with 50000 iterations where 10000 iterations were burned in. Runtime on the same desktop as in Section 3.1 was approximately 7 hours.

The left panel in Figure 6 compares the empirical cumulative distribution from river  $j = 1$  in January with its posterior cumulative distribution functions based on the MCMC runs. The right panel shows the corresponding probability - probability plots. These result indicate that the model describes the data well. Which in turn demonstrates that the MCMC split sampler recaptures the known underlying model, which was used to generate the simulated data. Analogous results hold across all rivers and months (results not shown).

Furthermore, as the data was generated from a known model setup, the results of the inference based on the MCMC runs can be compared to the known values of the model parameters. In Figure 7, the known values of the seasonal random effects are shown along with the corresponding 95% posterior intervals. The top panel in Figure 7 shows this comparison for the seasonal random effect  $u_{0,m,\lambda}$  for the log-location parameter  $\lambda$  as a function of months. The middle and the bottom panels in Figure 7 show the same comparison for  $u_{0,m,\tau}$  for the log-scale parameter and  $u_{0,m,\xi}$  for the shape parameter  $\xi$ , respectively. The results reveal that the 95% posterior intervals for the seasonal random effects contain their known values. These results demonstrate that the MCMC split sampler recaptures the known seasonal random effects. Similar results hold for all other model parameters (results now shown).

Gelman–Rubin plots and auto-correlation plots for nine model parameters based on the MCMC run are shown in Figures 8 and 9, respectively. Both plots are based on the same set of parameters and arranged identically. Three parameters were chosen from the location, scale and shape structures of the proposed model which were placed in the first, second and third rows of Figures 8 and 9, respectively. The first columns are based on parameters from the data-rich part of the latent field; the second columns are based on

parameters from the data-poor part of the latent field; and the third column is based on hyperparameters.

The Gelman–Rubin plots in Figure 8 show that the sampler has converged in the mean after roughly 10,000 iterations. Similar results hold for all the model parameters (results not shown). Furthermore, the autocorrelation plots in Figure 9 demonstrate that the MCMC chains for the parameters from both the data-rich and the data-poor parts of the latent field, exhibit a negligible autocorrelation after lag 10. The hyperparameters show a negligible autocorrelation after lag 30. Relying on these results, the MCMC chains exhibit all signs of having converged. Moreover, these results further indicate that the MCMC split sampler, with the modified proposal density of Roberts et al. [1997] implied by equation (3.9) for the hyperparameters, is highly computationally efficient in both the data-rich and data-poor blocks.

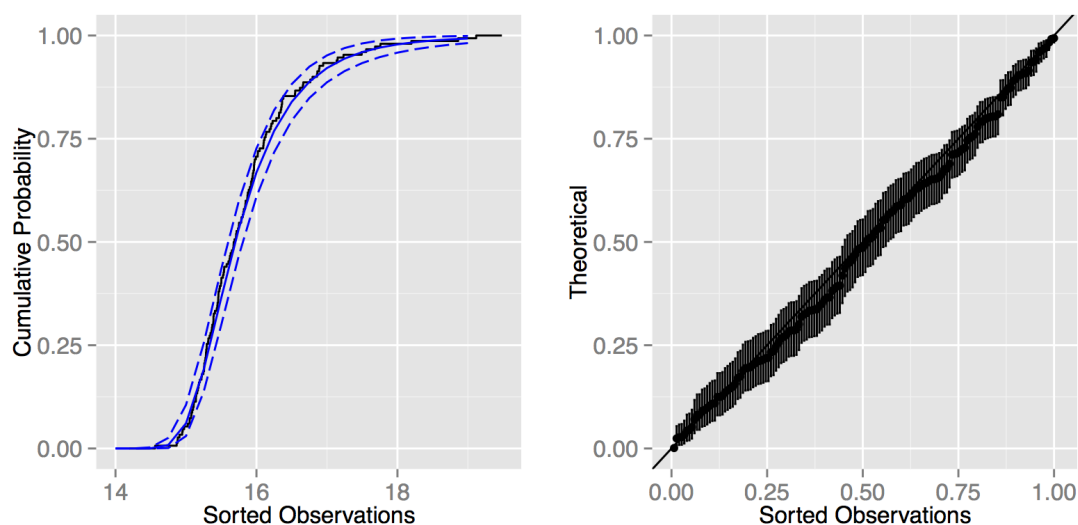


Figure 6: The left panel shows the empirical cumulative distribution of maximum instantaneous flow from river  $j = 1$  in January (black solid curve) and the posterior mean of the corresponding posterior cumulative distribution functions (blue solid curve) and corresponding 95% posterior interval (blue dashed curve). The right panel shows a probability-probability plot of maximum instantaneous flow from river  $j = 1$  in January, along with 95% posterior intervals.

## 4 Discussion

The main advantage (or novelty) of the MCMC split sampler lies in how the proposed blocking scheme leads to conditional posterior structures within in the two blocks, which can be exploited in order to construct computationally efficient sampling schemes for each block. Additionally, the MCMC split sampler is, in principle, designed as a modular

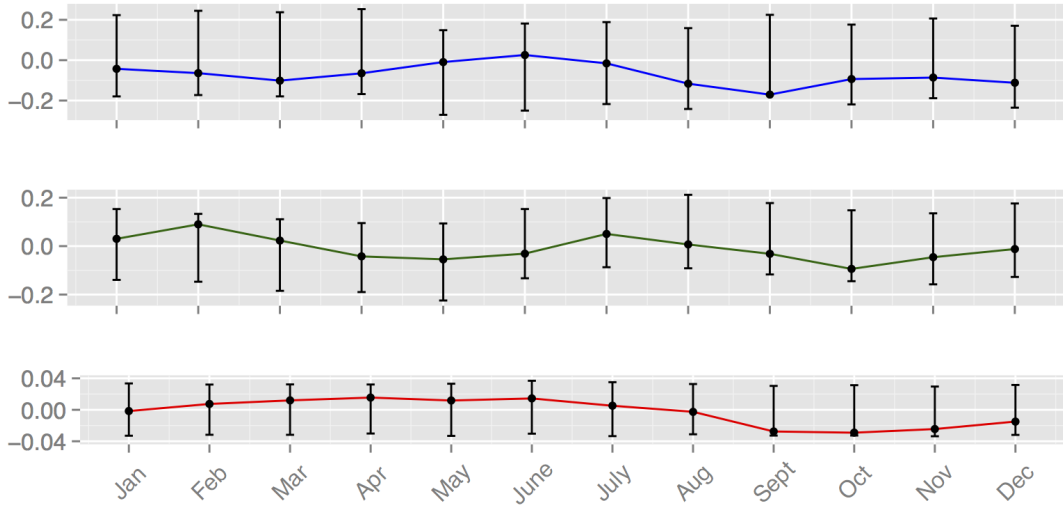


Figure 7: The top panel in shows the known value (denoted with the blue entries) of the seasonal random effect  $u_{0,m,\lambda}$  for the log-location parameter  $\lambda$  as function of months  $m$ . The middle panel shows the known value (denoted with the green entries) of the seasonal random effect  $u_{0,m,\tau}$  for log-scale parameter  $\tau$ . The bottom panel shows the known value (denoted with the red entries) of the seasonal random effect  $u_{0,m,\xi}$  for the shape parameter  $\xi$ . The errors bars in all panels represent the corresponding 95% posterior intervals based on the MCMC-runs.

sampling scheme in the sense that any MCMC sampling scheme can be implemented within the blocks. Therefore, in the authors' view, the MCMC split sampler presents an interesting area of future research as new sampling schemes for either block can be developed independently of the other block.

In the data-rich block, we proposed a Metropolis–Hastings algorithm with an independence proposal density which was constructed with a Gaussian approximation of the conditional posterior density evaluated at its mode. Furthermore, we proposed a modification the sampler which is applicable if conditional independence assumptions are imposed on the data density function. The modification can potentially increase the computational efficiency of the sampler, as discussed in Appendix A.

Although the proposed sampler in the data-rich block is computationally efficient, it is only applicable in practice if the mode of conditional posterior density function can be found, and can be calculated reasonably fast. For example, in the case of models where each observed data point has more than one unique data density parameters associated with it, say of the type  $y_i \sim \pi(y_i|\mu_i, \sigma_i)$  for every measurement  $i$ , finding the mode of the conditional posterior  $\pi(\mu_i, \sigma_i|y_i)$  becomes computationally impractical in some cases. Models of this type include, for example, certain spatial temporal models [Hrafnkelsson et al., 2012]. Similar computational issues also arise if data dependence at the data-level of a LGM is desired, see for example Davison et al. [2012] where t-copulas are implemented

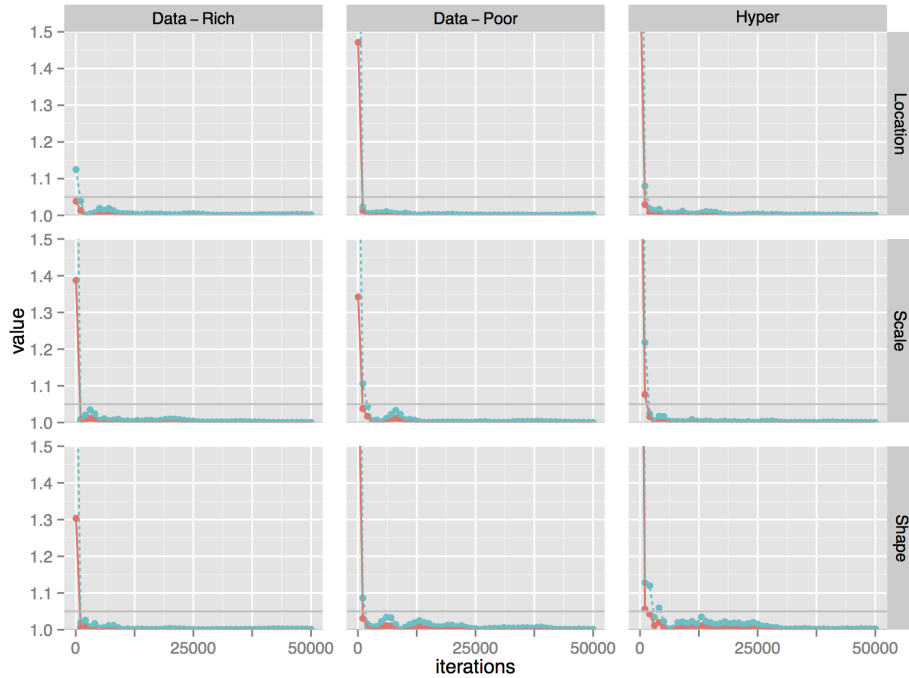


Figure 8: The figure shows Gelman–Rubin plots based on the MCMC run. The first, second and third rows in the first column are based on a randomly chosen log-location parameter  $\lambda$ ; covariate coefficient  $\beta_\lambda$ ; and hyperparameter  $\psi_\lambda$ , respectively. The second and third row show an analogous set of parameters based on the log-scale and shape structures, respectively, of the likelihood.

with g.e.v. marginal density functions at the data level as a model for spatial extremes. However, in both of the aforementioned cases different sampling scheme for the data-rich block can be implemented without changing the sampling scheme of choice in the data-poor block. For example, sampling scheme based on MALA and HMC type algorithm are well suited for the structure of the data-rich block in both cases.

In the data-poor block, the conditional posterior density  $\pi(\boldsymbol{\nu}|\boldsymbol{\eta}, \boldsymbol{\theta})$  is a Gaussian of the form (2.6) and invariant of the data density function. These results serves as one of the main computational advantage introduced by the MCMC split sampler due to the following reasons. First, as the conditional posterior  $\pi(\boldsymbol{\nu}|\boldsymbol{\eta}, \boldsymbol{\theta})$  is Gaussian, a modified version of the one block sampler of Knorr-Held and Rue [2002], which is known to be a highly efficient sampling scheme when applicable [Filippone et al., 2013], becomes applicable within the data-poor block regardless of the data-density function at the data level. As a consequence, computationally efficient sampling algorithms can be used to sample from the exact conditional posterior Gaussian density  $\pi(\boldsymbol{\nu}|\boldsymbol{\eta}, \boldsymbol{\theta})$ . Further, if the prior density functions in (2.4) have a sparse GMRF precision structure, then  $\pi(\boldsymbol{\nu}|\boldsymbol{\eta}, \boldsymbol{\theta})$  preserves the sparse structure as discussed in Section 2.4, which in turn allows for highly

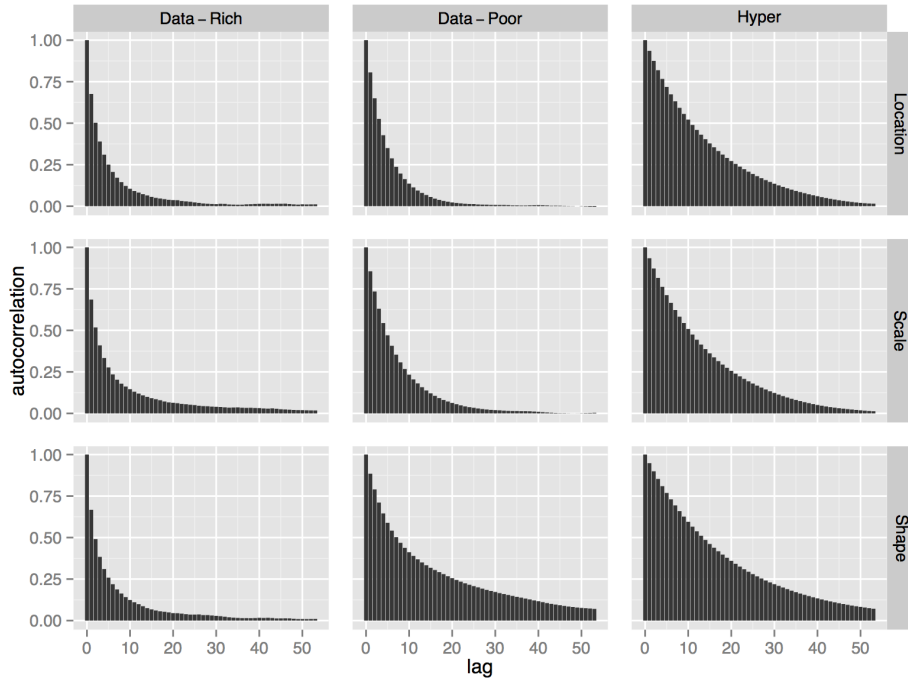


Figure 9: The figure shows auto-correlation plots based on the MCMC run. The first, second and third rows in the first column are based on a randomly chosen log-location parameter  $\lambda$ ; covariate coefficient  $\beta_\lambda$ ; and hyperparameter  $\psi_\lambda$ , respectively. The second and third row show an analogous set of parameters based on the log-scale and shape structures, respectively, of the likelihood.

efficient sampling algorithms for the Gaussian density  $\pi(\boldsymbol{\nu}|\boldsymbol{\eta}, \boldsymbol{\theta})$ . Therefore, the proposed sampling scheme in Section 2.4 for the data-poor blocks scales well in terms of computational speed and efficiency with increasing dimensions of the data-poor part of the latent field, which is of great importance to achieve, especially in the field of spatial statistics.

Second, as the conditional posterior density  $\pi(\boldsymbol{\nu}|\boldsymbol{\eta}, \boldsymbol{\theta})$  is a known Gaussian and the acceptance rate in the sampling scheme for the data-poor block in Section 2.4 is only dependent on hyperparameters, the computational efficiency of the proposed sampling scheme for the data-poor block is only dependent of the sampling scheme used for the hyperparameters. In this sense, the sampling scheme in Section 2.4 is in itself modular, that is, any proposal density for the hyperparameters is applicable. Choosing a computationally efficient sampling scheme for the hyperparameters can thus increase the computational efficiency of the overall sampling scheme within the data-poor block, as demonstrated in the examples in Section 3. That is, in Section 3.1 we demonstrated how a proposal density implied by equation (3.3) may be implemented due to its simplicity. However, in Section 3.2 we proposed a modified version of the sampling scheme of Roberts et al. [1997] implied by equation (3.9), which reduces the autocorrelation in

the MCMC chains. In practical terms, the proposal density implied by (3.9) can also be implemented Section 3.1, which in turn reduces the autocorrelation in the MCMC chains for the hyperparameters (results omitted).

Due to the modularity of the MCMC split sampler, sampling schemes for the data-rich block can be developed and improved independently of the sampler in the data-poor block, and vice versa. Additionally, as the conditional posterior density  $\pi(\nu|\eta, \theta)$  becomes invariant of the data in the data-poor block, the computational advantages introduced by the conditional posterior structure in the data-poor block hold for all LGMs. Moreover, the MCMC split sampler can be applied to various LGMs as it is designed to handle LGMs where latent models Gaussian models are imposed on more than just the mean structure of the data density function. Thus, in our view, further developing and improving sampling schemes that utilize the computational advantages introduced by the MCMC split sampler presents an interesting area of future research.

## Acknowledgements

The authors would like to thank the University of Iceland Doctoral Fund and University of Iceland Research Fund which supported the research. The authors would also like to thank the Icelandic Meteorological Office for providing the data. The authors give their thanks to the Nordic Network on Statistical Approaches to Regional Climate Models for Adaptation (SARMA), especially Prof. Peter Guttorp, for providing travel support. Furthermore, the authors give their thanks to the Department of Mathematical Sciences at the Norwegian University of Science and Technology for hosting Óli Páll Geirsson several times, and special gratitude to Prof. Håvard Rue for his invitation and valuable conversations.

## References

- George Casella and Edward I George. Explaining the gibbs sampler. *The American Statistician*, 46(3):167–174, 1992.
- Siddhartha Chib and Edward Greenberg. Understanding the metropolis-hastings algorithm. *The American Statistician*, 49(4):327–335, 1995.
- Daniel Cooley, Douglas Nychka, and Philippe Naveau. Bayesian spatial modeling of extreme precipitation return levels. *Journal of the American Statistical Association*, 102(479):824–840, 2007.
- Noel Cressie. *Statistics for spatial data*. 1993.
- Philippe Crochet, Tómas Jóhannesson, Trausti Jónsson, Oddur Sigurðsson, Helgi Björnsson, Finnur Pálsson, and Idar Barstad. Estimating the spatial distribution of precipitation in iceland using a linear model of orographic precipitation. *Journal of Hydrometeorology*, 8(6):1285–1306, 2007.

- Philippe Crochet et al. Estimating the flood frequency distribution for ungauged catchments using an index flood procedure. application to ten catchments in northern iceland. 2012.
- C Cunnane and J.E Nash. Bayesian estimation of frequency of hydrological events. *Proceedings of the Warsaw symposium. Mathematical models in hydrology*, 1(100):47–55, 1971.
- Anthony C Davison, SA Padoan, and Mathieu Ribatet. Statistical modeling of spatial extremes. *Statistical Science*, 27(2):161–186, 2012.
- Ólafur Birgir Davíðsson. Bayesian flood frequency analysis using monthly maxima. 2015.
- Pierre Delfiner et al. *Geostatistics: modeling spatial uncertainty*, volume 497. Wiley.com, 2009.
- Peter J Diggle, JA Tawn, and RA Moyeed. Model-based geostatistics. *Journal of the Royal Statistical Society: Series C (Applied Statistics)*, 47(3):299–350, 1998.
- Ludwig Fahrmeir, Gerhard Tutz, Wolfgang Hennevogl, and Eliane Salem. *Multivariate statistical modelling based on generalized linear models*, volume 2. Springer New York, 1994.
- M Filippone, M Zhong, and M Girolami. A comparative evaluation of stochastic-based inference methods for gaussian process models. *Machine Learning*, 2013.
- Óli P Geirsson, Birgir Hrafnkelsson, and Daniel Simpson. Computationally efficient spatial modeling of annual maximum 24-h precipitation on a fine grid. *Environmetrics*, 2015.
- Stuart Geman and Donald Geman. Stochastic relaxation, gibbs distributions, and the bayesian restoration of images. *Pattern Analysis and Machine Intelligence, IEEE Transactions on*, (6):721–741, 1984.
- Mark Girolami and Ben Calderhead. Riemann manifold langevin and hamiltonian monte carlo methods. *Journal of the Royal Statistical Society: Series B (Statistical Methodology)*, 73(2):123–214, 2011.
- GROUPE DE RECHERCHE ENHYDROLOGIE STATISTIQUE GREHY. Presentation and review of some methods for regional flood frequency analysis. *Journal of hydrology(Amsterdam)*, 186(1-4):63–84, 1996.
- Peter Guttorp and Tilmann Gneiting. Studies in the history of probability and statistics xlix on the matern correlation family. *Biometrika*, 93(4):989–995, 2006.
- W Keith Hastings. Monte carlo sampling methods using markov chains and their applications. *Biometrika*, 57(1):97–109, 1970.

- Birgir Hrafnkelsson, Jeffrey S Morris, and Veerabhadran Baladandayuthapani. Spatial modeling of annual minimum and maximum temperatures in iceland. *Meteorology and Atmospheric Physics*, 116(1-2):43–61, 2012.
- Thomas Kneib. Beyond mean regression. *Statistical Modelling*, 13(4):275–303, 2013.
- Leoanhard Knorr-Held and Håvard Rue. On block updating in markov random field models for disease mapping. *Scandinavian Journal of Statistics*, 29(4):597–614, 2002.
- Andrew B Lawson. *Bayesian disease mapping: hierarchical modeling in spatial epidemiology*. CRC Press, 2013.
- Finn Lindgren, Håvard Rue, and Johan Lindström. An explicit link between gaussian fields and gaussian markov random fields: The stochastic partial differential equation approach. *Journal of the Royal Statistical Society: Series B (Statistical Methodology)*, 73(4):423–498, 2011.
- Sara Martino, Kjersti Aas, Ola Lindqvist, Linda R Neef, and Håvard Rue. Estimating stochastic volatility models using integrated nested laplace approximations. *The European Journal of Finance*, 17(7):487–503, 2011.
- Thiago G Martins, Daniel Simpson, Janine B Illian, Håvard Rue, and Óli Páll Geirsson. Discussion of 'beyond mean regression'. *Statistical Modelling*, 13(4):355–361, 2013.
- Nicholas Metropolis, Arianna W Rosenbluth, Marshall N Rosenbluth, Augusta H Teller, and Edward Teller. Equation of state calculations by fast computing machines. *The journal of chemical physics*, 21:1087, 1953.
- Iain Murray and Ryan Prescott Adams. Slice sampling covariance hyperparameters of latent gaussian models. *arXiv preprint arXiv:1006.0868*, 2010.
- Radford M Neal. Probabilistic inference using markov chain monte carlo methods. 1993.
- Anthony N Pettitt, IS Weir, and AG Hart. A conditional autoregressive gaussian process for irregularly spaced multivariate data with application to modelling large sets of binary data. *Statistics and Computing*, 12(4):353–367, 2002.
- Gareth O Roberts and Jeffrey S Rosenthal. Optimal scaling of discrete approximations to langevin diffusions. *Journal of the Royal Statistical Society: Series B (Statistical Methodology)*, 60(1):255–268, 1998.
- Gareth O Roberts, Andrew Gelman, Walter R Gilks, et al. Weak convergence and optimal scaling of random walk metropolis algorithms. *The annals of applied probability*, 7(1):110–120, 1997.
- Håvard Rue. Fast sampling of gaussian markov random fields. *Journal of the Royal Statistical Society: Series B (Statistical Methodology)*, 63(2):325–338, 2001.

Havard Rue and Leonhard Held. *Gaussian Markov random fields: theory and applications*. CRC Press, 2005.

Håvard Rue, Sara Martino, and Nicolas Chopin. Approximate bayesian inference for latent gaussian models by using integrated nested laplace approximations. *Journal of the royal statistical society: Series b (statistical methodology)*, 71(2):319–392, 2009.

Bettina Schaefli, Daniela Balin Talamba, and André Musy. Quantifying hydrological modeling errors through a mixture of normal distributions. *Journal of Hydrology*, 332(3):303–315, 2007.

## Appendices

### A Conditionally independent data density functions

In many applications of LGMs, conditional independence assumptions are imposed on the likelihood function, see for example the discussion in Rue et al. [2009]. That is, by the model assumptions there exists a partition of  $\boldsymbol{\eta}$  into subvectors  $\boldsymbol{\eta}_i$ ,  $i = 1, \dots, I$ , such that

$$\pi(\mathbf{y} \mid \boldsymbol{\eta}) = \prod_{i=1}^I \pi_i(\mathbf{y}_i \mid \boldsymbol{\eta}_i) \quad (\text{A.1})$$

where  $\pi_i(\mathbf{y}_i \mid \boldsymbol{\eta}_i)$  denotes the marginal data density functions of the  $i$ -th partition. The conditional independence assumptions in (A.1) imply  $f(\boldsymbol{\eta}) = \sum_i f_i(\boldsymbol{\eta}_i)$ , where  $f_i$  is the logarithm of the marginal data density function  $\pi_i(\mathbf{y}_i \mid \boldsymbol{\eta}_i)$ . As discussed in Section 2.3, the Gaussian approximation in (2.9) can be, in some scenarios, a poor approximation of the conditional posterior density in some partition  $i$ , which in turn may cause the sampler to get stuck and thus lose its efficiency. To address this issue, we suggest a modified version of the sampler proposed in Section 2.3 which retains the computational speed gained by using a Gaussian approximation as a proposal density and is applicable if conditional independence assumptions are imposed on the data density function. Before we introduce the modifications to the sampling scheme in Section 2.3, we give a few essential technical results for the modifications, which are as follows.

**Lemma 6.** *Assuming the conditional independence assumptions in (A.1). Then, every pair of vectors  $\boldsymbol{\eta}_i$  and  $\boldsymbol{\eta}_{i'}$ , such that  $i \neq i'$ , become conditionally independent in the posterior given  $(\mathbf{y}, \boldsymbol{\nu}, \boldsymbol{\theta})$ . In other words, the following relation holds*

$$\pi(\boldsymbol{\eta}_i \mid \mathbf{y}, \boldsymbol{\eta}_{-i}, \boldsymbol{\nu}, \boldsymbol{\theta}) = \pi(\boldsymbol{\eta}_i \mid \mathbf{y}, \boldsymbol{\nu}, \boldsymbol{\theta}) \quad (\text{A.2})$$

for all partitions  $i$ . Furthermore, the conditional posterior density of  $\boldsymbol{\eta}_i$  is independent of  $\mathbf{y}_{-i}$ , which denotes the subvector of the data vector  $\mathbf{y}$  that is not observed in partition

*i*. That is, the following relationship holds

$$\pi(\boldsymbol{\eta}_i \mid \mathbf{y}, \boldsymbol{\nu}, \boldsymbol{\theta}) = \pi(\boldsymbol{\eta}_i \mid \mathbf{y}_i, \boldsymbol{\nu}, \boldsymbol{\theta}) \quad (\text{A.3})$$

for all partitions *i*

For notational simplicity and based on the relation in (A.2) and (A.3), we denote the conditional posterior density of  $\boldsymbol{\eta}_i$  with  $\pi_i(\boldsymbol{\eta}_i \mid \mathbf{y}, \boldsymbol{\nu}, \boldsymbol{\theta})$  henceforth. The following corollary yields a useful identity for the conditional posterior  $\boldsymbol{\eta}_i$  with  $\pi_i(\boldsymbol{\eta}_i \mid \mathbf{y}, \boldsymbol{\nu}, \boldsymbol{\theta})$ .

**Corollary 7.** *Assume the conditional independence assumptions in (A.1). The logarithm of the conditional posterior density  $\pi_i(\boldsymbol{\eta}_i \mid \mathbf{y}, \boldsymbol{\nu}, \boldsymbol{\theta})$  is*

$$\log \pi_i(\boldsymbol{\eta}_i \mid \mathbf{y}, \boldsymbol{\nu}, \boldsymbol{\theta}) = f_i(\boldsymbol{\eta}_i) - \frac{1}{2} \boldsymbol{\eta}_i^\top \mathbf{Q}_{\epsilon, (i,i)} \boldsymbol{\eta}_i + \left( \mathbf{Q}_{\epsilon, (i,i)} (\mathbf{Z}\boldsymbol{\nu})_i \right)^\top \boldsymbol{\eta}_i + K \quad (\text{A.4})$$

where  $K$  is a constant.

The subsequent corollary is the immediate from Theorem 2, Lemma 6 and the relation in (A.4).

**Corollary 8.** *Assuming the conditional independence assumptions in (A.1), the Gaussian approximation of the conditional posterior  $\pi_i(\boldsymbol{\eta}_i \mid \mathbf{y}, \boldsymbol{\nu}, \boldsymbol{\theta})$  within each partition *i* is*

$$\tilde{\pi}_i(\boldsymbol{\eta}_i \mid \mathbf{y}, \boldsymbol{\theta}, \boldsymbol{\nu}) = \mathcal{N} \left( \boldsymbol{\eta}_i \mid \boldsymbol{\eta}_i^0, (\mathbf{Q}_\epsilon - \mathbf{H})_{(i,i)} \right) \quad (\text{A.5})$$

where  $\boldsymbol{\eta}_i^0$  denotes the mode of the marginal posterior density function  $\pi_i(\boldsymbol{\eta}_i \mid \mathbf{y}, \boldsymbol{\nu}, \boldsymbol{\theta})$  and  $(\mathbf{Q}_\epsilon - \mathbf{H})_{(i,i)}$  denotes the submatrix of  $(\mathbf{Q}_\epsilon - \mathbf{H})$  belonging to partition *i*.

The next corollary shows the relation between the Gaussian approximation density functions in (2.9) and (A.5).

**Corollary 9.** *Assume the conditional independence assumptions in (A.1). Furthermore, let  $\tilde{\pi}(\boldsymbol{\eta} \mid \mathbf{y}, \boldsymbol{\nu}, \boldsymbol{\theta})$  denote the Gaussian approximation of the conditional posterior density  $\pi(\boldsymbol{\eta} \mid \mathbf{y}, \boldsymbol{\nu}, \boldsymbol{\theta})$ , and  $\tilde{\pi}_i(\boldsymbol{\eta}_i \mid \mathbf{y}, \boldsymbol{\nu}, \boldsymbol{\theta})$  denote the Gaussian approximation of the conditional posterior  $\pi_i(\boldsymbol{\eta}_i \mid \mathbf{y}, \boldsymbol{\nu}, \boldsymbol{\theta})$  within partition *i*. Then the following relation holds*

$$\tilde{\pi}(\boldsymbol{\eta} \mid \mathbf{y}, \boldsymbol{\nu}, \boldsymbol{\theta}) = \prod_i^I \tilde{\pi}_i(\boldsymbol{\eta}_i \mid \mathbf{y}, \boldsymbol{\nu}, \boldsymbol{\theta}). \quad (\text{A.6})$$

The modifications to the sampler proposed in Section 2.3 are based on the following observations. From the conditional posterior independence relation in (A.2) in Lemma 6 follows directly

$$\pi(\boldsymbol{\eta}_i \mid \mathbf{y}, \boldsymbol{\eta}_{-i}, \boldsymbol{\nu}, \boldsymbol{\theta}) = \pi(\boldsymbol{\eta}_i \mid \mathbf{y}, \boldsymbol{\nu}, \boldsymbol{\theta})$$

for all partitions *i*. It is therefore equivalent to update  $\boldsymbol{\eta}_i \mid \mathbf{y}, \boldsymbol{\eta}_{-i}, \boldsymbol{\nu}, \boldsymbol{\theta}$  iteratively over partitions *i*, with a Gibbs sampling approach using (A.5) as a proposal density and

to update  $\boldsymbol{\eta}_i | \mathbf{y}, \boldsymbol{\nu}, \boldsymbol{\theta}$  separately over partitions  $i$ . By updating separately as opposed to iteratively, the number of function calls is reduced, which in turn reduces computational cost.

However, in practical terms it is faster to compute the mode once by computing the maximum of  $\log \pi(\boldsymbol{\eta} | \mathbf{y}, \boldsymbol{\nu}, \boldsymbol{\theta})$  than computing the maximum of  $\log \pi_i(\boldsymbol{\eta}_i | \mathbf{y}, \boldsymbol{\nu}, \boldsymbol{\theta})$  separately in every partition  $i$ . This is due to the fact that number of function calls increases as  $I$  increases in the numerical optimizing methods when finding the mode of  $\log \pi_i(\boldsymbol{\eta}_i | \mathbf{y}, \boldsymbol{\nu}, \boldsymbol{\theta})$  within every partition  $i$ . Furthermore, the computational cost of calculating the function  $\log \pi(\boldsymbol{\eta} | \mathbf{y}, \boldsymbol{\nu}, \boldsymbol{\theta})$  in (2.8) is minimal and scales well as the dimension of the data-poor block increases, as the  $\mathbf{Q}_\epsilon$  is a diagonal matrix and  $\mathbf{Z}$  is a fixed sparse matrix. Thus, calculating the gradient and the Hessian matrix of the conditional posterior is also computationally feasible in many cases.

The relation in (A.6) demonstrates that it is equivalent to propose a new vector  $\boldsymbol{\eta}^*$  from the normal approximation  $\tilde{\pi}(\boldsymbol{\eta} | \mathbf{y}, \boldsymbol{\nu}, \boldsymbol{\theta})$  and to propose new vectors  $\boldsymbol{\eta}_i^*$  separately from  $\tilde{\pi}_i(\boldsymbol{\eta}_i | \mathbf{y}, \boldsymbol{\nu}, \boldsymbol{\theta})$  for every  $i$ . Therefore, to reduce computational cost and to increase computational efficiency, we propose the following modifications to the sampling scheme in Section 2.3. That is, propose a new vector  $\boldsymbol{\eta}^*$  from  $q(\boldsymbol{\eta}) = \tilde{\pi}(\boldsymbol{\eta} | \mathbf{y}, \boldsymbol{\nu}, \boldsymbol{\theta})$  and accept and reject  $\boldsymbol{\eta}_i^*$  within each partition separately with the probability

$$\alpha_i = \min \left\{ 1, \frac{\pi(\boldsymbol{\eta}_i^* | \mathbf{y}, \boldsymbol{\nu}, \boldsymbol{\theta})}{\tilde{\pi}(\boldsymbol{\eta}_i^* | \mathbf{y}, \boldsymbol{\nu}, \boldsymbol{\theta})} \bigg/ \frac{\pi(\boldsymbol{\eta}_i^k | \mathbf{y}, \boldsymbol{\nu}, \boldsymbol{\theta})}{\tilde{\pi}(\boldsymbol{\eta}_i^k | \mathbf{y}, \boldsymbol{\nu}, \boldsymbol{\theta})} \right\}. \quad (\text{A.7})$$

The acceptance ratio in (A.7) can be calculated separately over partitions  $i$  with a low computational cost, as demonstrated in the following corollary.

**Corollary 10.** *Assume the conditional independence assumptions in (A.1) and adopt the same notation as in Lemma 3. The logarithm of the acceptance ratio in (A.7), that is*

$$r_i = \log \left( \frac{\pi(\boldsymbol{\eta}_i^* | \mathbf{y}, \boldsymbol{\nu}, \boldsymbol{\theta})}{\tilde{\pi}(\boldsymbol{\eta}_i^* | \mathbf{y}, \boldsymbol{\nu}, \boldsymbol{\theta})} \bigg/ \frac{\pi(\boldsymbol{\eta}_i^k | \mathbf{y}, \boldsymbol{\nu}, \boldsymbol{\theta})}{\tilde{\pi}(\boldsymbol{\eta}_i^k | \mathbf{y}, \boldsymbol{\nu}, \boldsymbol{\theta})} \right)$$

where  $\tilde{\pi}_i(\boldsymbol{\eta}_i | \mathbf{y}, \boldsymbol{\nu}, \boldsymbol{\theta})$  denotes the Gaussian approximation of the conditional posterior  $\pi_i(\boldsymbol{\eta}_i | \mathbf{y}, \boldsymbol{\nu}, \boldsymbol{\theta})$  within partition  $i$ . Then  $r_i$  can be simplified to

$$r_i = f_i(\boldsymbol{\eta}_i^*) + \boldsymbol{\rho}(\boldsymbol{\eta}^*)_i^\top \mathbf{1} - (f_i(\boldsymbol{\eta}_i^k) + \boldsymbol{\rho}(\boldsymbol{\eta}^k)_i^\top \mathbf{1})$$

for all  $i$ , where  $f_i$  is the logarithm of the marginal data density function in partition  $i$  and

$$\boldsymbol{\rho}(\boldsymbol{\eta}) = \left( \frac{1}{2} \boldsymbol{\eta}^\top \mathbf{H} + \mathbf{b}^\top \right) \circ \boldsymbol{\eta}$$

for notational simplicity, where  $\circ$  denotes an entrywise multiplication. The corresponding acceptance probability in partition  $i$  is thus

$$\alpha_i = \min \{ 1, \exp r_i \}.$$

The sampling scheme for the data-rich block with the aforementioned modifications is summarised in Algorithm 2

## B Proofs

### B.1 Proof of Lemma 1

*Proof.* By know results about Gaussian distributions and inverses of block matrices, the joint distribution of  $(\boldsymbol{\eta}, \boldsymbol{\nu})$  is given by

$$\begin{aligned}\pi\left(\begin{matrix} \boldsymbol{\eta} \\ \boldsymbol{\nu} \end{matrix}\right) &= \mathcal{N}\left(\begin{pmatrix} \boldsymbol{\eta} \\ \boldsymbol{\nu} \end{pmatrix} \middle| \begin{pmatrix} \mathbf{Z}\boldsymbol{\mu}_\nu \\ \boldsymbol{\mu}_\nu \end{pmatrix}, \begin{pmatrix} \mathbf{Q}_\epsilon & -\mathbf{Q}_\epsilon\mathbf{Z} \\ -\mathbf{Z}^\top\mathbf{Q}_\epsilon & \mathbf{Q}_\nu + \mathbf{Z}^\top\mathbf{Q}_\epsilon\mathbf{Z} \end{pmatrix}^{-1}\right) \\ &= \mathcal{N}\left(\begin{pmatrix} \boldsymbol{\eta} \\ \boldsymbol{\nu} \end{pmatrix} \middle| \begin{pmatrix} \mathbf{Z}\boldsymbol{\mu}_\nu \\ \boldsymbol{\mu}_\nu \end{pmatrix}, \begin{pmatrix} \mathbf{Q}_\epsilon^{-1} + \mathbf{Z}\mathbf{Q}_\nu^{-1}\mathbf{Z}^\top & \mathbf{Z}\mathbf{Q}_\nu^{-1} \\ \mathbf{Q}_\nu^{-1}\mathbf{Z}^\top & \mathbf{Q}_\nu^{-1} \end{pmatrix}\right)\end{aligned}$$

The conditional distribution  $\boldsymbol{\nu}$  conditioned on  $\boldsymbol{\eta}$  follows directly from Lemma 2.1 in [Rue and Held, 2005], that is,

$$\pi(\boldsymbol{\nu} \mid \boldsymbol{\eta}) = \mathcal{N}\left(\boldsymbol{\nu} \mid \mathbf{Q}_{\nu|\eta}^{-1}(\mathbf{Q}_\nu\boldsymbol{\mu}_\nu + \mathbf{Z}^\top\mathbf{Q}_\epsilon\boldsymbol{\eta}), \mathbf{Q}_{\nu|\eta}^{-1}\right)$$

where  $\mathbf{Q}_{\nu|\eta} = \mathbf{Q}_\nu + \mathbf{Z}^\top\mathbf{Q}_\epsilon\mathbf{Z}$ . □

### B.2 Proof of Theorem 2

*Proof.* The conditional posterior density function  $\pi(\boldsymbol{\eta} \mid \mathbf{y}, \boldsymbol{\nu}, \boldsymbol{\theta})$  is proportional to the product of the data density function and the conditional Gaussian prior density  $\pi(\boldsymbol{\eta} \mid \boldsymbol{\nu}, \boldsymbol{\theta})$  given by (2.4), that is

$$\pi(\boldsymbol{\eta} \mid \mathbf{y}, \boldsymbol{\nu}, \boldsymbol{\theta}) \propto \pi(\mathbf{y} \mid \boldsymbol{\eta})\pi(\boldsymbol{\eta} \mid \boldsymbol{\nu}, \boldsymbol{\theta}).$$

Thus, the logarithm of the conditional posterior density function is given by

$$\log \pi(\boldsymbol{\eta} \mid \mathbf{y}, \boldsymbol{\nu}, \boldsymbol{\theta}) = f(\boldsymbol{\eta}) - \frac{1}{2}\boldsymbol{\eta}^\top\mathbf{Q}_\epsilon\boldsymbol{\eta} + (\mathbf{Q}_\epsilon\mathbf{Z}\boldsymbol{\nu})^\top\boldsymbol{\eta} + \text{const}$$

where  $f(\boldsymbol{\eta}) = \log \pi(\mathbf{y} \mid \boldsymbol{\eta})$  for notational convenience. The second order Taylor approximation of  $f(\boldsymbol{\eta})$  expanded around the mode  $\boldsymbol{\eta}^0$  of the conditional posterior  $\pi(\boldsymbol{\eta} \mid \mathbf{y}, \boldsymbol{\nu}, \boldsymbol{\theta})$  is

$$\begin{aligned}f(\boldsymbol{\eta}) &\approx f(\boldsymbol{\eta}^0) + \nabla f(\boldsymbol{\eta}^0)^\top(\boldsymbol{\eta} - \boldsymbol{\eta}^0) + \frac{1}{2}(\boldsymbol{\eta} - \boldsymbol{\eta}^0)^\top\mathbf{H}(\boldsymbol{\eta} - \boldsymbol{\eta}^0) \\ &= \frac{1}{2}\boldsymbol{\eta}^\top\mathbf{H}\boldsymbol{\eta} + (\nabla f(\boldsymbol{\eta}^0) - \mathbf{H}\boldsymbol{\eta}^0)^\top\boldsymbol{\eta} + \text{const}.\end{aligned}$$

Consequently, the second order Taylor approximation of  $\log \pi(\boldsymbol{\eta} \mid \mathbf{y}, \boldsymbol{\nu}, \boldsymbol{\theta})$  expanded around  $\boldsymbol{\eta}^0$  becomes

$$\begin{aligned}\log \pi(\boldsymbol{\eta} \mid \mathbf{y}, \boldsymbol{\nu}, \boldsymbol{\theta}) &\approx \frac{1}{2}\boldsymbol{\eta}^\top\mathbf{H}\boldsymbol{\eta} + (\nabla f(\boldsymbol{\eta}^0) - \mathbf{H}\boldsymbol{\eta}^0)^\top\boldsymbol{\eta} - \frac{1}{2}\boldsymbol{\eta}^\top\mathbf{Q}_\epsilon\boldsymbol{\eta} + (\mathbf{Q}_\epsilon\mathbf{Z}\boldsymbol{\nu})^\top\boldsymbol{\eta} + \text{const} \\ &= -\frac{1}{2}\boldsymbol{\eta}^\top(\mathbf{Q}_\epsilon - \mathbf{H})\boldsymbol{\eta} + (\mathbf{Q}_\epsilon\mathbf{Z}\boldsymbol{\nu} + \mathbf{b})^\top\boldsymbol{\eta} + \text{const},\end{aligned}$$

where  $\mathbf{b} = (\nabla f(\boldsymbol{\eta}^0) - \mathbf{H}\boldsymbol{\eta}^0)$ . This derivation yields a Gaussian approximation with a mean vector

$$(\mathbf{Q}_\epsilon - \mathbf{H})^{-1} (\mathbf{Q}_\epsilon \mathbf{Z}\boldsymbol{\nu} + \mathbf{b})$$

and covariance matrix  $(\mathbf{Q}_\epsilon - \mathbf{H})^{-1}$ . However, as the vector  $\boldsymbol{\eta}^0$  is the mode of the conditional posterior function  $\pi(\boldsymbol{\eta} \mid \mathbf{y}, \boldsymbol{\nu}, \boldsymbol{\theta})$  the following relation holds

$$\nabla \log \pi(\boldsymbol{\eta}^0 \mid \mathbf{y}, \boldsymbol{\nu}, \boldsymbol{\theta}) = \nabla f(\boldsymbol{\eta}^0) - \mathbf{Q}_\epsilon \boldsymbol{\eta}^0 + (\mathbf{Q}_\epsilon \mathbf{Z}\boldsymbol{\nu})^\top = \mathbf{0}.$$

The mean of the Gaussian approximations becomes

$$\begin{aligned} & (\mathbf{Q}_\epsilon - \mathbf{H})^{-1} (\mathbf{Q}_\epsilon \mathbf{Z}\boldsymbol{\nu} + \mathbf{b}) \\ &= (\mathbf{Q}_\epsilon - \mathbf{H})^{-1} (\mathbf{Q}_\epsilon \mathbf{Z}\boldsymbol{\nu} + \nabla f(\boldsymbol{\eta}^0) - \mathbf{H}\boldsymbol{\eta}^0) \\ &= (\mathbf{Q}_\epsilon - \mathbf{H})^{-1} (\mathbf{Q}_\epsilon \boldsymbol{\eta}^0 - \mathbf{H}\boldsymbol{\eta}^0) \\ &= (\mathbf{Q}_\epsilon - \mathbf{H})^{-1} (\mathbf{Q}_\epsilon - \mathbf{H})\boldsymbol{\eta}^0 = \boldsymbol{\eta}^0 \end{aligned}$$

Thus, a Gaussian approximation of the conditional posterior density function  $\pi(\boldsymbol{\eta} \mid \mathbf{y}, \boldsymbol{\nu}, \boldsymbol{\theta})$  evaluated at the mode  $\boldsymbol{\eta}^0$  is given by

$$\tilde{\pi}(\boldsymbol{\eta} \mid \mathbf{y}, \boldsymbol{\nu}, \boldsymbol{\theta}) = \mathcal{N}(\boldsymbol{\eta} \mid \boldsymbol{\eta}^0, (\mathbf{Q}_\epsilon - \mathbf{H})^{-1}).$$

□

### B.3 Proof of Lemma 3

*Proof.* The logarithm of the acceptance ratio given in (2.10) is

$$r = \log \frac{\pi(\boldsymbol{\eta}^* \mid \mathbf{y}, \boldsymbol{\nu}, \boldsymbol{\theta})q(\boldsymbol{\eta}^k)}{\pi(\boldsymbol{\eta}^k \mid \mathbf{y}, \boldsymbol{\nu}, \boldsymbol{\theta})q(\boldsymbol{\eta}^*)} \quad (\text{B.1})$$

where  $\pi(\boldsymbol{\eta} \mid \mathbf{y}, \boldsymbol{\nu}, \boldsymbol{\theta})$  is the conditional posterior density function given in (2.4) and  $q(\boldsymbol{\eta})$  is the proposal density based on the Gaussian approximation in (2.9). The right hand side term in (B.1) can be written as

$$\begin{aligned} & \log \pi(\boldsymbol{\eta}^* \mid \mathbf{y}, \boldsymbol{\nu}, \boldsymbol{\theta}) - \log q(\boldsymbol{\eta}^*) \\ & - \left( \log \pi(\boldsymbol{\eta}^k \mid \mathbf{y}, \boldsymbol{\nu}, \boldsymbol{\theta}) + \log q(\boldsymbol{\eta}^k) \right) \end{aligned}$$

Since the proposal density  $q$  is based on the Gaussian approximation in (2.9) the following holds

$$\begin{aligned} \log \pi(\boldsymbol{\eta} \mid \mathbf{y}, \boldsymbol{\nu}, \boldsymbol{\theta}) - \log q(\boldsymbol{\eta}) &= f(\boldsymbol{\eta}) - \frac{1}{2} \boldsymbol{\eta}^\top \mathbf{Q}_\epsilon \boldsymbol{\eta} + (\mathbf{Q}_\epsilon \mathbf{Z}\boldsymbol{\nu})^\top \boldsymbol{\eta} \\ & - \left( \frac{1}{2} \boldsymbol{\eta}^\top \mathbf{H} \boldsymbol{\eta} + \mathbf{b}^\top \boldsymbol{\eta} - \frac{1}{2} \boldsymbol{\eta}^\top \mathbf{Q}_\epsilon \boldsymbol{\eta} + (\mathbf{Q}_\epsilon \mathbf{Z}\boldsymbol{\nu})^\top \boldsymbol{\eta} \right) + \text{const} \\ &= f(\boldsymbol{\eta}) - \left( \frac{1}{2} \boldsymbol{\eta}^\top \mathbf{H} \boldsymbol{\eta} + \mathbf{b}^\top \boldsymbol{\eta} \right) + \text{const} \end{aligned}$$

which yields the results in (2.11). □

## B.4 Proof of Lemma 4

*Proof.* By definition of the proposal density in (2.13) the following holds

$$\frac{q(\boldsymbol{\nu}^k, \boldsymbol{\theta}^k | \boldsymbol{\nu}^*, \boldsymbol{\theta}^*)}{q(\boldsymbol{\nu}^*, \boldsymbol{\theta}^* | \boldsymbol{\nu}^k, \boldsymbol{\theta}^k)} = \frac{\pi(\boldsymbol{\nu}^k | \boldsymbol{\eta}^{k+1}, \boldsymbol{\theta}^k) q(\boldsymbol{\theta}^k | \boldsymbol{\theta}^*)}{\pi(\boldsymbol{\nu}^* | \boldsymbol{\eta}^{k+1}, \boldsymbol{\theta}^*) q(\boldsymbol{\theta}^* | \boldsymbol{\theta}^k)},$$

where  $q(\boldsymbol{\theta}^* | \boldsymbol{\theta}^k)$  is some proposal density for  $\boldsymbol{\theta}$  and  $\pi(\boldsymbol{\nu} | \boldsymbol{\eta}, \boldsymbol{\theta})$  is the conditional Gaussian density function in (2.6) in Lemma 1. Therefore, the acceptance ratio in (2.14) can be written as

$$\frac{\pi(\boldsymbol{\nu}^*, \boldsymbol{\theta}^* | \mathbf{y}, \boldsymbol{\eta}^{k+1}) \pi(\boldsymbol{\nu}^k | \boldsymbol{\eta}^{k+1}, \boldsymbol{\theta}^k) q(\boldsymbol{\theta}^k | \boldsymbol{\theta}^*)}{\pi(\boldsymbol{\nu}^k, \boldsymbol{\theta}^k | \mathbf{y}, \boldsymbol{\eta}^{k+1}) \pi(\boldsymbol{\nu}^* | \boldsymbol{\eta}^{k+1}, \boldsymbol{\theta}^*) q(\boldsymbol{\theta}^* | \boldsymbol{\theta}^k)} = \frac{\pi(\boldsymbol{\theta}^* | \boldsymbol{\eta}^{k+1}) q(\boldsymbol{\theta}^k | \boldsymbol{\theta}^*)}{\pi(\boldsymbol{\theta}^k | \boldsymbol{\eta}^{k+1}) q(\boldsymbol{\theta}^* | \boldsymbol{\theta}^k)} \quad (\text{B.2})$$

since  $\pi(\boldsymbol{\nu}, \boldsymbol{\theta} | \mathbf{y}, \boldsymbol{\eta}) = \pi(\boldsymbol{\nu}, \boldsymbol{\theta} | \boldsymbol{\eta})$ , as discussed in Section 2.4, and  $\pi(\boldsymbol{\nu}, \boldsymbol{\theta} | \boldsymbol{\eta}) / \pi(\boldsymbol{\nu} | \boldsymbol{\eta}, \boldsymbol{\theta}) = \pi(\boldsymbol{\theta} | \boldsymbol{\eta})$  for any  $\boldsymbol{\eta}, \boldsymbol{\nu}$  and  $\boldsymbol{\theta}$ . The result in (B.2) demonstrates that the acceptance ratio in (2.14) is only dependant on  $\boldsymbol{\theta}$  within in the proposed setup. In other words, the acceptance ratio in (2.14) becomes independent of the value of  $\boldsymbol{\nu}$ .  $\square$

## B.5 Proof of Theorem 5

*Proof.* In order to rewrite  $\pi(\boldsymbol{\theta} | \boldsymbol{\eta})$  in (2.15) we use the relation

$$\pi(\boldsymbol{\theta} | \boldsymbol{\eta}) \propto \pi(\boldsymbol{\theta}) \pi(\boldsymbol{\eta} | \boldsymbol{\theta}). \quad (\text{B.3})$$

Further, by the law of conditional probability, the following holds

$$\pi(\boldsymbol{\eta} | \boldsymbol{\theta}) = \frac{\pi(\boldsymbol{\eta}, \boldsymbol{\nu} | \boldsymbol{\theta})}{\pi(\boldsymbol{\nu} | \boldsymbol{\eta}, \boldsymbol{\theta})} = \frac{\pi(\boldsymbol{\eta} | \boldsymbol{\nu}, \boldsymbol{\theta}) \pi(\boldsymbol{\nu} | \boldsymbol{\theta})}{\pi(\boldsymbol{\nu} | \boldsymbol{\eta}, \boldsymbol{\theta})} \quad (\text{B.4})$$

As  $\pi(\boldsymbol{\eta} | \boldsymbol{\theta})$  is independent of the value of  $\boldsymbol{\nu}$ , it follows that the two ratios in (B.4) are invariant of the choice of  $\boldsymbol{\nu}$ . In particular, the following holds

$$\pi(\boldsymbol{\eta} | \boldsymbol{\theta}) = \frac{\pi(\boldsymbol{\eta} | \mathbf{0}, \boldsymbol{\theta}) \pi(\mathbf{0} | \boldsymbol{\theta})}{\pi(\mathbf{0} | \boldsymbol{\eta}, \boldsymbol{\theta})} \quad (\text{B.5})$$

by choosing the value  $\boldsymbol{\nu} = \mathbf{0}$ . Combining (B.3) and (B.5) yields

$$\begin{aligned} \frac{\pi(\boldsymbol{\theta}^* | \boldsymbol{\eta}^{k+1})}{\pi(\boldsymbol{\theta}^k | \boldsymbol{\eta}^{k+1})} &= \frac{\pi(\boldsymbol{\theta}^*) \pi(\boldsymbol{\eta}^{k+1} | \boldsymbol{\theta}^*)}{\pi(\boldsymbol{\theta}^k) \pi(\boldsymbol{\eta}^{k+1} | \boldsymbol{\theta}^k)} \\ &= \frac{\pi(\boldsymbol{\theta}^*)}{\pi(\boldsymbol{\theta}^k)} \times \frac{\pi(\boldsymbol{\eta}^{k+1} | \mathbf{0}, \boldsymbol{\theta}^*) \pi(\mathbf{0} | \boldsymbol{\theta}^*)}{\pi(\mathbf{0} | \boldsymbol{\eta}^{k+1}, \boldsymbol{\theta}^*)} \times \frac{\pi(\mathbf{0} | \boldsymbol{\eta}^{k+1}, \boldsymbol{\theta}^k)}{\pi(\boldsymbol{\eta}^{k+1} | \mathbf{0}, \boldsymbol{\theta}^k) \pi(\mathbf{0} | \boldsymbol{\theta}^k)}. \end{aligned}$$

Moreover, if the Gaussian prior density functions in (2.4) are GMRFs with sparse precision structures, then all of the conditional density functions on the rightmost side of (B.4) are GMRFs with sparse precision structures, by known results about conditioning on subvectors as demonstrated in Theorem 2.5 in Rue and Held [2005].  $\square$

## B.6 Proof of Lemma 6

*Proof.* As the matrix  $\mathbf{Q}_\epsilon$  is a diagonal matrix the following holds

$$\begin{aligned}\pi(\boldsymbol{\eta} \mid \boldsymbol{\nu}, \boldsymbol{\theta}) &= \mathcal{N}(\boldsymbol{\eta} \mid \mathbf{Z}\boldsymbol{\nu}, \mathbf{Q}_\epsilon^{-1}) \\ &= \prod_{i=1}^I \mathcal{N}(\boldsymbol{\eta}_i \mid (\mathbf{Z}\boldsymbol{\nu})_i, \mathbf{Q}_{\epsilon, (i,i)}^{-1})\end{aligned}\tag{B.6}$$

where  $\mathbf{Q}_{\epsilon, (i,i)}$  denotes the submatrix of  $\mathbf{Q}_\epsilon$  belonging to partition  $i$ . Let

$$\pi_i(\boldsymbol{\eta}_i \mid \boldsymbol{\nu}, \boldsymbol{\theta}) = \mathcal{N}(\boldsymbol{\eta}_i \mid (\mathbf{Z}\boldsymbol{\nu})_i, \mathbf{Q}_{\epsilon, (i,i)}^{-1})$$

which serves as the conditional prior density function for the data-rich part of the latent field belonging to partition  $i$ . The relation in (B.6) along with the conditional independence assumptions in (A.1) yield

$$\begin{aligned}\pi(\boldsymbol{\eta} \mid \mathbf{y}, \boldsymbol{\nu}, \boldsymbol{\theta}) &\propto \pi(\mathbf{y} \mid \boldsymbol{\eta})\pi(\boldsymbol{\eta} \mid \boldsymbol{\nu}, \boldsymbol{\theta}) \\ &= \prod_{i=1}^I \pi_i(\mathbf{y}_i \mid \boldsymbol{\eta}_i)\pi_i(\boldsymbol{\eta}_i \mid \boldsymbol{\nu}, \boldsymbol{\theta})\end{aligned}$$

which demonstrates that the vectors  $\boldsymbol{\eta}_i$  and  $\boldsymbol{\eta}_{i'}$  are conditionally independent in the conditional posterior given  $(\mathbf{y}, \boldsymbol{\nu}, \boldsymbol{\theta})$ , for all  $i \neq i'$ .

Furthermore, the conditional independence assumptions in (A.1) also yield

$$\begin{aligned}\pi(\boldsymbol{\eta}_i \mid \mathbf{y}, \boldsymbol{\nu}, \boldsymbol{\theta}) &\propto \pi(\mathbf{y}_i \mid \boldsymbol{\eta}_i)\pi_i(\boldsymbol{\eta}_i \mid \boldsymbol{\nu}, \boldsymbol{\theta}) \\ &\propto \pi(\boldsymbol{\eta}_i \mid \mathbf{y}_i, \boldsymbol{\nu}, \boldsymbol{\theta})\end{aligned}\tag{B.7}$$

which demonstrates that  $\pi(\boldsymbol{\eta}_i \mid \mathbf{y}, \boldsymbol{\nu}, \boldsymbol{\theta})$  is independent of  $\mathbf{y}_{-i}$ .  $\square$

## B.7 Proof of Corollary 7

*Proof.* The conditional independence assumptions in (A.1), the relation in (B.6) and the relation in (B.7) yield

$$\begin{aligned}\log \pi_i(\boldsymbol{\eta}_i \mid \mathbf{y}_i, \boldsymbol{\nu}, \boldsymbol{\theta}) &= \log \pi(\mathbf{y}_i \mid \boldsymbol{\eta}_i) + \log \pi_i(\boldsymbol{\eta}_i \mid \boldsymbol{\nu}, \boldsymbol{\theta}) + K \\ &= f_i(\boldsymbol{\eta}_i) - \frac{1}{2}\boldsymbol{\eta}_i^\top \mathbf{Q}_{\epsilon, (i,i)} \boldsymbol{\eta}_i + \left(\mathbf{Q}_{\epsilon, (i,i)}(\mathbf{Z}\boldsymbol{\nu})_i\right)^\top \boldsymbol{\eta}_i + K\end{aligned}$$

for every partition  $i$ .  $\square$

## B.8 Proof of Corollary 8

*Proof.* The result follows by using Theorem 2 on the  $\log \pi_i(\boldsymbol{\eta}_i \mid \mathbf{y}, \boldsymbol{\nu}, \boldsymbol{\theta})$  given in (A.4) instead of  $\log \pi(\boldsymbol{\eta} \mid \mathbf{y}, \boldsymbol{\nu}, \boldsymbol{\theta})$ .  $\square$

## B.9 Proof of Corollary 9

*Proof.* The relation in (A.2) and (A.3) in Lemma (6) implies that the elements of mode  $\boldsymbol{\eta}^0$  belonging to partition  $i$  are also the mode of  $\pi_i(\boldsymbol{\eta}_i | \mathbf{y}_i, \boldsymbol{\nu}, \boldsymbol{\theta})$  in every partition  $i$ . The results then follows from Lemma 6, Theorem 2 and Corollary 8.  $\square$

## B.10 Proof of Corollary 10

*Proof.* As conditional independence are imposed over partitions  $i$ , Lemma 6 yields the following

$$\begin{aligned} \log \pi(\boldsymbol{\eta} | \mathbf{y}, \boldsymbol{\theta}, \boldsymbol{\nu}) - \log \tilde{\pi}(\boldsymbol{\eta} | \mathbf{y}, \boldsymbol{\nu}, \boldsymbol{\theta}) &= f(\boldsymbol{\eta}) - \frac{1}{2} \boldsymbol{\eta}^\top \mathbf{H} \boldsymbol{\eta} - \mathbf{b}^\top \boldsymbol{\eta} + \text{const} \\ &= \sum_i \left( f_i(\boldsymbol{\eta}_i) - \frac{1}{2} \boldsymbol{\eta}_i^\top \mathbf{H}_{(i,i)} \boldsymbol{\eta}_i - \mathbf{b}_i^\top \boldsymbol{\eta}_i \right) + \text{const}. \end{aligned}$$

The results follows by similar derivations as in the proof of Lemma 3.  $\square$